Block Catiomer Polyplexes with Regulated Densities of Charge and Disulfide Cross-Linking Directed To Enhance Gene Expression

Kanjiro Miyata, Yoshinori Kakizawa, Nobuhiro Nishiyama, Atsushi Harada, Yuichi Yamasaki, Hiroyuki Koyama, and Kazunori Kataoka

Contribution from the Department of Materials Science and Engineering, Graduate School of Engineering, The University of Tokyo, 7-3-1 Hongo, Bunkyo-ku, Tokyo 113-8656, Japan, National Institute for Materials Science, 1-1 Namiki, Tsukuba, Ibaraki 305-0044, Japan, and Department of Clinical Vascular Regeneration, Graduate School of Medicine, The University of Tokyo, 7-3-1 Hongo, Bunkyo-ku, Tokyo 113-8655, Japan

JOURNAL OF THE AMERICAN CHEMICAL SOCIETY®

Reprinted from
Volume 126, Number 8, Pages 2355–2361

J|A|C|S
ARTICLES
Published on Web 02/06/2004

Block Catiomer Polyplexes with Regulated Densities of Charge and Disulfide Cross-Linking Directed To Enhance Gene Expression

Kanjiro Miyata,[†] Yoshinori Kakizawa,[‡] Nobuhiro Nishiyama,[†,§] Atsushi Harada,[†] Yuichi Yamasaki,[†] Hiroyuki Koyama,[§] and Kazunori Kataoka*[,†,‡]

Contribution from the Department of Materials Science and Engineering, Graduate School of Engineering, The University of Tokyo, 7-3-1 Hongo, Bunkyo-ku, Tokyo 113-8656, Japan, National Institute for Materials Science, 1-1 Namiki, Tsukuba, Ibaraki 305-0044, Japan, and Department of Clinical Vascular Regeneration, Graduate School of Medicine, The University of Tokyo, 7-3-1 Hongo, Bunkyo-ku, Tokyo 113-8655, Japan

Received August 16, 2003; E-mail: kataoka@bmw.t.u-tokyo.ac.jp

Abstract: A block catiomer polyplex, showing a high stability in the extracellular medium and an efficient release of plasmid DNA (pDNA) in the intracellular compartment, was developed by controlling both the cationic charge and disulfide cross-linking densities of the backbone polycations. Poly(ethylene glycol)-poly(L-lysine) block copolymer (PEG-PLL) was thiolated using either of two thiolation reagents, *N*-succinimidyl 3-(2-pyridyldithio)propionate (SPDP) or 2-iminothiolane (Traut's reagent), to investigate the effects of both the charge and disulfide cross-linking densities on the properties of the polyplexes. The introduction of thiol groups by SPDP proceeded through the formation of amide linkages to concomitantly decrease the cationic charge density of PLL segment, whereas Traut's reagent promoted the thiolation with the introduction of cationic imino groups to keep the charge density constant. These thiolated PEG-PLLs were complexed with pDNA to form the disulfide cross-linked block catiomer polyplexes, which had the size of approximately 100 nm. Both thiolation methods were similarly effective in introducing disulfide cross-links to prevent the polyplex from the dissociation through a counter polyanion exchange in the extracellular oxidative condition. On the other hand, the efficient release of pDNA responding to the reductive condition mimicking the intracellular environment was only achieved for the polyplex thiolated with SPDP, a system compensating for the decrease in the charge density with the disulfide cross-linking. This distinctive sensitivity toward oxidative and reductive environments was nicely correlated with the remarkable difference in the transfection efficiency between these two types of thiolated polyplexes (SPDP and Traut's reagent types): the former revealed approximately 50 times higher transfection efficiency toward 293T cells than the latter. Obviously, the balance between the densities of the cationic charge and disulfide cross-linking in the thiolated polyplex played a crucial role in the delivery and controlled release of entrapped pDNA into the microenvironment of intracellular compartment to achieve the high transfection efficiency.

Introduction

Despite the current enormous interest in cationic polymer-based gene delivery systems (polyplexes), the rationale to design efficient systems has not yet been obtained. Especially, in vivo gene delivery systems through a systemic route demand a high stability during blood circulation and an efficient gene expression at the target site. Cationic block copolymers with hydrophilic segments, such as poly(ethylene glycol) (PEG), effectively induce a condensation of plasmid DNA (pDNA) upon complexation to form core−shell-type polyplexes with the hydrophilic outer layer surrounding the polyion complex (PIC) core.[1−5] This provides the increased colloidal stability to the polyplexes in a proteinaceous medium, allowing the substantial increase in their blood circulation time.[3] Nevertheless, there is still a possibility of the block catiomer polyplexes to unfavorably dissociate before entering the cytoplasm of target cells through the interaction with negatively charged biomacromolecules in the entity.[6,7] Thus, a strategy is needed to keep the polyplex structure stable in the extracytoplasmic environment, while inducing the efficient release of entrapped pDNA from the polyplexes after their movement into the cytoplasmic compartment.

† Graduate School of Engineering, The University of Tokyo.
‡ National Institute for Materials Science.
§ School of Medicine, The University of Tokyo.

(1) (a) Katayose, S.; Kataoka, K. *Advanced Biomaterials in Biomedical Engineering and Drug Delivery Systems*; Springer: Tokyo, 1996; pp 319−320. (b) Katayose, S.; Kataoka, K. *Bioconjugate Chem.* **1997**, *8*, 702−707.
(2) Wolfert, M. A.; Schacht, E. H.; Toncheva, V.; Ulbrich, K.; Nazarova, O.; Seymour, L. W. *Hum. Gene Ther.* **1996**, *7*, 2123−2133.
(3) Harada-Shiba, M.; Yamauchi, K.; Harada, A.; Takamisawa, I.; Shimokado, K.; Kataoka, K. *Gene Ther.* **2002**, *9*, 407−414.
(4) Kakizawa, Y.; Kataoka, K. *Adv. Drug Delivery Rev.* **2002**, *54*, 203−222.
(5) Kwok, K. Y.; McKenzie, D. L.; Evers, D. L.; Rice, K. G. *J. Pharm. Sci.* **1999**, *88*, 996−1003.
(6) Oupicky, D.; Howard, K. A.; Konak, C.; Dash, P. R.; Ulbrich, K.; Seymour, L. W. *Bioconjugate Chem.* **2000**, *11*, 492−501.
(7) Oupicky, D.; Carlisle, R. C.; Seymour, L. W. *Gene Ther.* **2001**, *8*, 713−724.

10.1021/ja0379666 CCC: $27.50

Scheme 1. Thiolation Schemes of PEG-PLL

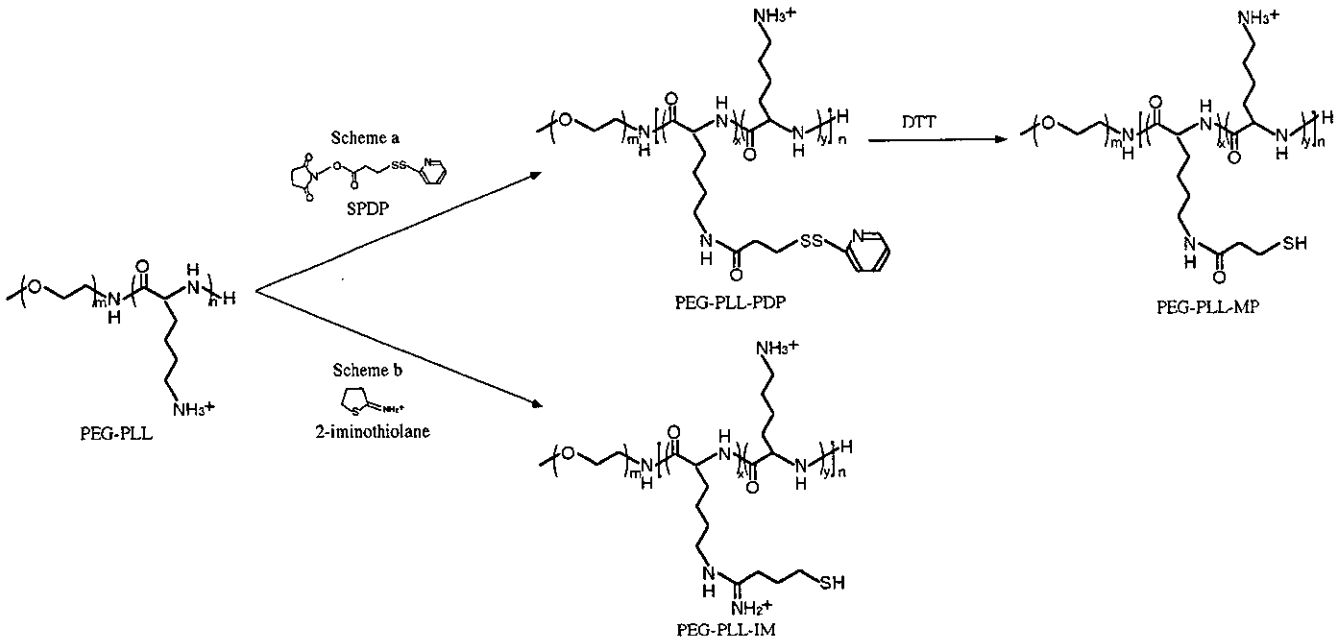

A promising approach to realize this strategy is to reversibly cross-link the PIC core of the block catiomer polyplex with disulfide bonds cleavable in intracellular reductive environments, where the glutathione concentration is ~50−1000 times higher than that in extracellular milieu.[8] Indeed, the utility of this strategy was demonstrated with the PIC of model polyanions,[9] oligo-DNA,[10] and pDNA,[7,11,12] showing that the disulfide cross-linking substantially stabilized polyplexes to achieve longevity in the blood circulation. However, the introduction of disulfide cross-links eventually led to the decreased transfection efficiency because of the overstabilization of the complex structure to hinder pDNA release in the intracellular compartment.[11] In this regard, the balance between cationic charge and disulfide cross-linking densities of the polyplex should be crucial for the disulfide cross-linked polyplexes achieving the environment-sensitive release of entrapped pDNA in the cytoplasm while maintaining its high stability in an extracellular environment. Nevertheless, previous works regarding the disulfide cross-linking of the polyplexes have not clarified this important issue, directing us to the present study devoting to design the polyplex system with regulated densities of charge and disulfide cross-linking to achieve the enhanced gene expression.

Here the charge and disulfide cross-linking densities of block catiomer polyplexes from PEG-poly(L-lysine) block copolymer (PEG-PLL) were regulated by the use of two types of thiolation reagents: *N*-succinimidyl 3-(2-pyridyldithio)propionate (SPDP)[13] and 2-iminothiolane (Traut's reagent).[14] Thiolation using SPDP proceeds by substituting amide groups for the ϵ-amino groups of the lysine residue, resulting in the decreased charge density compensated by the introduction of 3-(2-pyridyldithio)propionyl groups, while the charge density of the PLL segments remained unchanged even after thiolation by Traut's reagent, because the reaction was accompanied by the introduction of cationic imino groups. Consequently, the former system, balancing the densities of charge and disulfide cross-linking, achieved for the first time a remarkable increase in the transfection efficiency compared to non-cross-linked control while maintaining its stability in the extracellular environment.

Experimental Section.

Materials. α-Methoxy-ω-amino-poly(ethylene glycol) (M_w = 12 000) was a kind gift from Nippon Oil and Fats Co., Ltd. (Tokyo, Japan). The PEG-PLL block copolymers with an average polymerization degree of PLL segment of 71 were synthesized as previously described.[4] *N*-Succinimidyl 3-(2-pyridyldithio)propionate (SPDP), dithiothreitol (DTT), and sodium dextran sulfate (M_w = 25 000) were purchased from Wako Pure Chemical Co., Ltd. (Osaka, Japan). 2-Iminothiolane (Traut's reagent) and Micro BCA protein assay reagent kit were purchased from PIERCE Co., Inc. (Rockford, IL). *N*-Methyl-2-pyrrolidone (NMP) was purchased from Aldrich Co., Inc. (Milwaukee, WI). A pGL3 control vector, which was purchased from Promega Co., Inc. (Madison, WI), was used as pDNA in all the experiments. This pDNA was amplified in competent DH5α *Escherichia coli* and purified using HiSpeed Plasmid MaxiKit purchased from QIAGEN Sciences Co., Inc. (Germantown, MD).

Synthesis of Thiolated PEG-PLL. Introduction of thiol groups to the side chain of PEG-PLL was performed using either a heterobifunctional reagent SPDP[13] (Scheme 1a) or a cyclic thioimidate Traut's reagent[14] (Scheme 1b). The typical synthetic procedure is described as follows for the PEG-PLL-PDP (37 mol % substitution): PEG-PLL (51 mg, 1.90 μmol) and SPDP (60 mg, 192 μmol) were separately dissolved in NMP containing 5 wt % LiCl (2 mL for PEG-PLL, 6 mL for SPDP). The solution containing SPDP (2.5 mL) was added to PEG-PLL solution (2 mL) and stirred at room temperature for 24 h after the addition of 10% volume of *N*,*N*-diisopropylethylamine. Then, the mixture was precipitated into an approximately 20-times-excess volume of diethyl ether. The crude precipitate was washed twice with diethyl ether to

(8) Meister, A.; Anderson, M. E. *Annu. Rev. Biochem.* **1983**, *52*, 711−760.
(9) Kakizawa, Y.; Harada, A.; Kataoka, K. *J. Am. Chem. Soc.* **1999**, *121*, 11247−11248.
(10) Kakizawa, Y.; Harada, A.; Kataoka, K. *Biomacromolecules* **2001**, *2*, 491−497.
(11) Trubetskoy, S. V.; Loomis, A.; Slattum, M. P.; Hagstrom, E. J.; Budker, G. V.; Wolff, A. J. *Bioconjugate Chem.* **1999**, *10*, 624−628.
(12) McKenzie, D. L.; Kwok, K. Y.; Rice, K. G. *J. Biol. Chem.* **2000**, *275*, 9970−9977.
(13) Carlsson, J.; Drevin, H.; Axen, R. *Biochem. J.* **1978**, *173*, 723−737.
(14) King, T. P.; Li, Y.; Kochoumian, L. *Prepr. Protein Conjugates* **1978**, *17*, 1499−1506.

obtain white powder. The polymer was dissolved in 0.01 N HCl solution, dialyzed against distilled water overnight, and lyophilized to obtain the final product. The reaction of PEG-PLL with Traut's reagent was carried out in a similar way, e.g., Traut's reagent (20 mg, 145 μmol) in NMP (2 mL) was added to PEG-PLL (29 mg, 1.10 μmol) in NMP (2 mL) to obtain the PEG-PLL-IM (22 mol % substitution). Thiolated PEG-PLLs with different thiolation degrees were obtained by changing molar ratio of SPDP or Traut's reagent to the ϵ-amino groups of PEG-PLL according to the aforementioned method. The degree of the thiol substitution for each thiolated PEG-PLL was determined from the peak intensity ratio of the methylene protons of PEG (OCH_2CH_2, δ = 3.5 ppm) to the pyridyl protons of the 3-(2-pyridyldithio)propionyl groups (C_5H_4N, δ = 7.2−8.3 ppm) or the newly introduced methylene protons of 1-imino-4-mercaptobutyl groups ($HS-(CH_2)_3-C(NH_2^+)^-$, δ = 2.1−3.4 ppm) in ^{1}H NMR spectra taken in D_2O at 25 °C.

Preparation of the Cross-Linked Block Catiomer Polyplex. Each thiolated PEG-PLL was dissolved in 10 mM Tris-HCl buffer (pH 7.4) at 1−2 mg/mL, followed by the addition of 10% volume of 100 mM DTT solution. After a 30 min incubation at room temperature, the polymer solutions were diluted up to the residual molar concentration of the cationic moieties (primary amino and imino groups) to equal 0.615 μmol/mL by the same buffer. Then, the polymer solutions were added to a 2-times-excess volume of 50 μg/mL pDNA solution (0.154 μmol/mL phosphate groups) to form the polyplex at a charge ratio of 2. The final concentration of pDNA in all the samples was adjusted to 33 μg/mL. Charge ratio was defined as the residual molar ratio of positive charge of PEG-PLL or thiolated PEG-PLL to phosphate group of pDNA. After an overnight incubation at room temperature, the polyplex solutions were dialyzed against 10 mM Tris-HCl (pH 7.4) containing 0.5% dimethyl sulfoxide at 37 °C for 24 h to remove the impurities, followed by 2 days of additional dialysis for removal of dimethyl sulfoxide. During the dialysis, the thiol groups of thiolated PEG-PLL were oxidized to form the disulfide cross-links. To follow the process of oxidation, the remaining thiol groups in disulfide cross-linked polyplexes were determined by Ellman's method.[15]

Size of Cross-Linked Block Catiomer Polyplex. To estimate the hydrodynamic diameters of cross-linked block catiomer polyplexes, dynamic light scattering (DLS) measurements were carried out using a DLS-7000 instrument (Otuka Electronics Co, Ltd., Hirakata, Japan). An Ar ion laser (λ = 488 nm) was used as an incident beam. Block catiomer polyplex solutions with a charge ratio of 2 were adjusted to have a concentration of 33 μg pDNA/mL. The data obtained at a detection angle of 90° at 25 °C were analyzed by the cumulant method to obtain the hydrodynamic diameters and polydispersity indices (μ/Γ^2) of the polyplexes.[16]

For AFM imaging of DNA complexes, 4 μL of each sample solution was deposited on a freshly cleaved mica substrate for 30 s. The solution was dried under a gentle flow of nitrogen gas. AFM imaging was performed in tapping mode with standard silicon probes (160 μm in length, Olympus, Tokyo, Japan) on a NVB100 microscope (Olympus) controlled by an operating software of Nanoscope IIIa (Digital Instruments, Santa Barbara, CA). Cantilever oscillation frequency was tuned to the resonance frequency of the cantilever, 260−340 kHz. The 256 × 256 images were recorded at a 0.5−2 μm/s linear scanning speed at a sampling density of 4−60 nm^2 per pixel. Raw AFM images have been processed only for background removal (flattening) using the microscope manufacturer's image-processing software.

Dye Exclusion Assay. Block catiomer polyplex solutions (33 μg pDNA/mL) prepared at a charge ratio of 2 were adjusted to have 10 μg pDNA/mL with 2.5 μg EtBr/mL and 150 mM NaCl by adding 10 mM Tris-HCl (pH 7.4) buffer containing EtBr and NaCl. The solutions were incubated at ambient temperature overnight. Fluorescence measurements of sample solutions were carried out at 25 °C using a spectrofluorometer (FP-6500, Jasco, Tokyo, Japan). Fluorescence intensity of the samples at 590 nm was measured with excitation at 510 nm. Relative fluorescence intensity was calculated as follows:

$$F_r = (F_{sample} - F_0)/(F_{100} - F_0)$$

where F_{sample} was fluorescence intensity for the samples, F_{100} was free pDNA, and F_0 was background.

Gel Retardation Analysis. Sodium dextran sulfate (0.83 mM, M_w = 25 000) in 10 mM Tris-HCl (pH 7.4) buffer was added to the same volume of polyplex solutions (33 μg pDNA/mL) prepared at a charge ratio of 2 in 10 mM Tris-HCl (pH 7.4) buffer to have an approximately 20-times-excess charge ratio of sodium dextran sulfate to pDNA in the mixture. The mixed solution was then diluted up to 8.3 μg pDNA/mL by the same volume of 10 mM Tris-HCl (pH 7.4) buffer with or without 50 mM DTT. After an overnight incubation at 37 °C in a sealed container, 20 μL of each sample (166 ng pDNA) was electrophoresed at 100 V for 1 h on a 0.9 wt % agarose gel in 20 mM Tris-acetic acid buffer containing 10 mM sodium acetic acid (pH 7.8). pDNA in the gel was visualized by EtBr (0.5 μg/mL) staining.

Transfection. 293T cells were plated into six well gelatin-coated culture plates. After a 24 h incubation in 1.5 mL of Dulbecco's modified eagle medium (DMEM) containing 10% serum, the medium was replaced with 1 mL of a transfection medium containing 10% serum and 100 μM hydroxychloroquine. Ninety μL of each polyplex solution (33 μg/mL pDNA) was then applied to each well for the transfection. The amount of pDNA was adjusted to 3 μg per well. After 24 h of incubation, the medium was replaced with 1 mL of the medium containing 10% serum, followed by an additional 24 h incubation. The luciferase gene expression was then evaluated from the intensity of photoluminescence using Fluoroskan Ascent FL system (Labsystems, Helsinki, Finland). The amount of protein in each well was concomitantly determined using a Micro BCA Protein Assay Reagent Kit.

Effect of Freeze−Thawing Process of Polyplexes on Transfection. Polyplex solutions with a charge ratio of 2 were prepared as described in the preceding section to adjust the pDNA concentration of 33 μg/mL. Each sample was frozen at −20 °C for 2 h, followed by thawing at room temperature for 30 min. Both nonfrozen and freeze−thawed polyplexes were subjected to the luciferase transfection assay using 293T cells.

Results and Discussion

Thiolation of PEG-PLL. Thiolated PEG-PLLs were synthesized using two types of thiolation reagents, i.e., SPDP and Traut's reagent. The activated ester of SPDP reacts with the ϵ-amino group of lysine residue, resulting in the introduction of the 3-(2-pyridyldithio)propionyl (PDP) groups via amide linkage into the side chain of the PLL segment of PEG-PLL (Scheme 1a). Consequently, the cationic charge density of the PLL segment was decreased through the thiolation. Samples with varying thiolation degree were prepared by this method and abbreviated as PDP-X, where X stands for the percent thiolation (%) of the ϵ-amino groups calculated from the peak intensity ratio of the methylene protons of PEG (OCH_2CH_2, δ = 3.5 ppm) to the pyridyl protons of the 3-(2-pyridyldithio)-propionyl groups (C_5H_4N, δ = 7.2−8.3 ppm) in ^{1}H NMR spectrum as typically seen in Figure 1 (PDP-37). Treatment of PDP-X with an excess amount of DTT gave the reduced form having flanking 3-mercaptopropionyl groups, which we abbreviated as MP-X.

As an approach of thiolation with keeping the charge density unchanged, the amidination of ϵ-amino groups of PLL segment

(15) Riddles, P. W.; Blakeley, R. L.; Zerner, B. *Anal. Biochem.* **1979**, *94*, 75−81.
(16) Itaka, K.; Yamauchi, K.; Harada, A.; Nakamura, K.; Kawaguchi, H.; Kataoka, K. *Biomaterials* **2003**, *24*, 4495−4506.

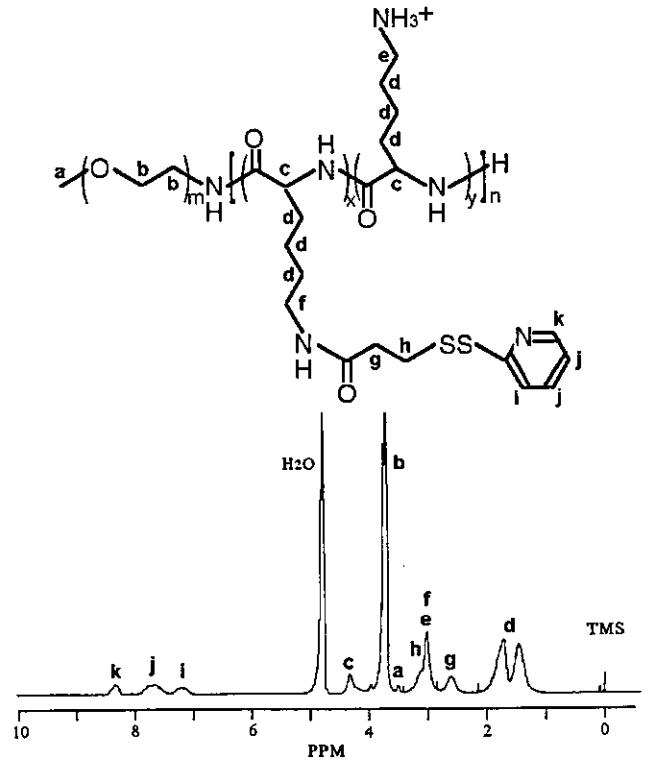

Figure 1. ^{1}H NMR spectrum of PDP-37 (solvent, D_2O; temperature, 25 °C; concentration, 10 mg/mL).

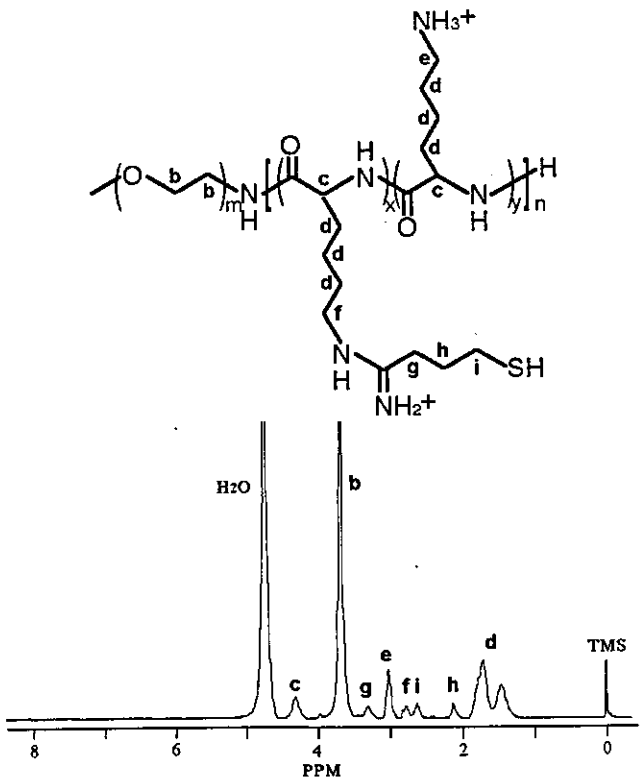

Figure 2. ^{1}H NMR spectrum of IM-22 (solvent, D_2O; temperature, 25 °C; concentration, 10 mg/mL).

was done by Traut's reagent to introduce thiol groups with cationic imino moieties as seen in Scheme 1b. ^{1}H NMR spectrum shown in Figure 2 (IM-22) clearly indicates the introduction of both thiol and imino moieties in the sample from the peaks of newly introduced methylene protons of 1-imino-4-mercaptobutyl groups from Traut's reagent ($HS-(CH_2)_3-C(NH_2^+)^-$, $\delta = 2.1-3.4$ ppm). Thiolated polymers containing 1-imino-4-mercaptobutyl groups were abbreviated as IM-X, where X stands for the percent thiolation.

Table 1. Cumulant Diameters and Polydispersity Indices (μ/Γ^2) of Block Catiomer Polyplexes

	cumulant diameter [nm]	polydispersity index (μ/Γ^2)
PEG-PLL polyplex (non-cross-linked)	102	0.16
IM-X polyplexes (cross-linked)		
IM-9	102	0.15
IM-22	100	0.16
MP-X polyplexes (cross-linked)		
MP-5	103	0.14
MP-13	106	0.14
MP-28	103	0.13
MP-37	115	0.19

Formation of Cross-Linked Block Catiomer Polyplex. The block catiomer polyplexes from pDNA and thiolated PEG-PLL were prepared at the charge ratio of 2, where no free pDNA was observed in an agarose gel retardation analysis (data not shown). To determine the process of oxidative cross-linking, the polyplex samples were subjected to Ellman's test for the estimation of residual thiol groups. After 3 days of dialysis, the amount of remaining thiol groups was calculated to be less than 10% of the initial value for all the samples, indicating that the core of block catiomer polyplexes was cross-linked through covalent disulfide bonds between the side chain of PLL segment of PEG-PLL.

The size and shape of the cross-linked polyplexes were then evaluated by DLS and AFM measurements. Table 1 summarizes the cumulant diameters of the polyplexes determined by DLS, indicating that all of the block catiomer polyplexes, regardless of the cross-linking and charge densities, have diameters around 100 nm with a moderate polydispersity between 0.13 and 0.19. This is in line with the results of the atomic force microscopy (AFM) of the dried polyplexes on a mica disk as seen in Figure 3. A toroidal structure in the size range of 60−100 nm and a rodlike structure with a long axis of 150−300 nm were observed by AFM. Our previous work on polyplex examination by static light scattering revealed that the block catiomer polyplexes of PEG-PLL prepared at a charge ratio of 2 is likely to contain a single pDNA molecule in each of the polyplexes without any secondary coalescence.[16] Present AFM imaging of the polyplexes is reasonably consistent with this previous estimation based on the static light scattering analysis.

Ethidium bromide (EtBr) is known to form an intercalating complex with double helical polynucleotides to show a striking enhancement in its fluorescence intensity.[17] This enhanced fluorescence was quenched upon the condensation of DNA through the complexation with cationic component due to the hindered intercalation of EtBr into double-stranded structure of DNA molecules. Thus, EtBr exclusion assay was frequently utilized to estimate the degree of pDNA condensation in ion complexes.[17,18] As seen in Figure 4, non-cross-linked polyplexes

(17) LePecq, J.-B.; Paoletti, C. *J. Mol. Biol.* **1967**, *27*, 87−106.
(18) Itaka, K.; Harada, A.; Nakamura, K.; Kawaguchi, H.; Kataoka, K. *Biomacromolecules* **2002**, *3*, 841−845.

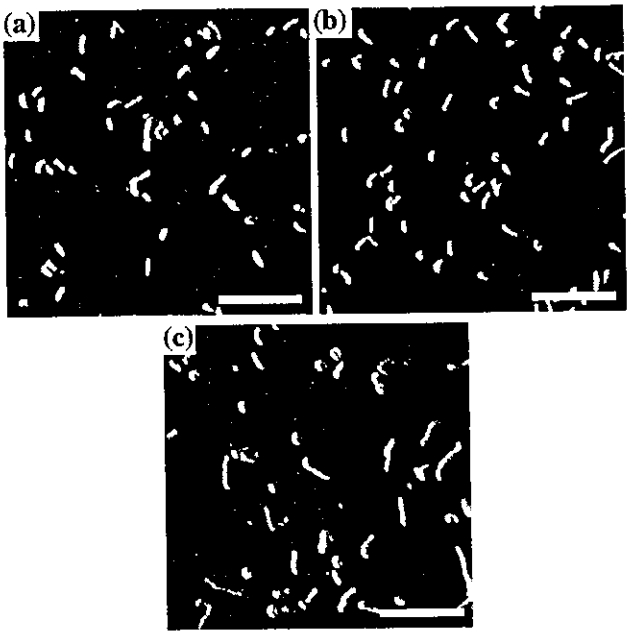

Figure 3. AFM images of block catiomer polyplexes. (a) PEG-PLL polyplex (non-cross-linked), (b) IM-22 polyplex (cross-linked), and (c) MP-28 polyplex (cross-linked). Images are shown in amplitude mode, and all the scale bars are equivalent to 500 nm.

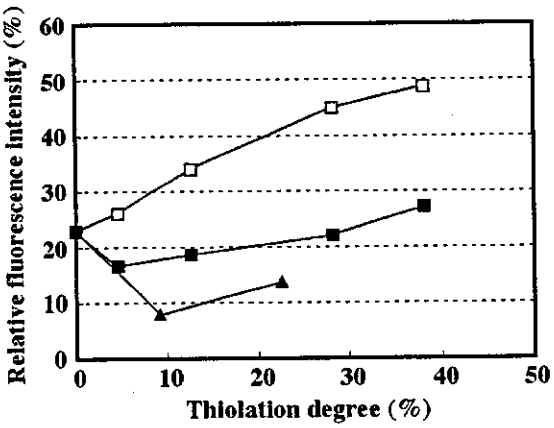

Figure 4. Effect of thiolation degree of non-cross-linked and cross-linked block catiomer polyplexes on the fluorescence intensity of EtBr. Fluorescence measurements were carried out as described in the Experimental Section. (□) PDP-X polyplex, (■) MP-X polyplex, (▲) IM-X polyplex.

from PDP-X showed a monotonic increase in the EtBr fluorescence with an increase in the thiolation degree, indicating a lowered tendency of dye exclusion. This result demonstrates that the decreased charge density of PLL segment through the reaction with SPDP led to a lowered capacity to induce pDNA condensation. On the other hand, the disulfide cross-linked polyplexes from MP-X had a substantially lowered fluorescence intensity than the corresponding non-cross-linked polyplexes from PDP-X and revealed the fluorescence intensity the same as the polyplex from PEG-PLL (nonthiolated polymer), indicating their characteristic to compensate for the decreased cationic charge with disulfide cross-linking. Furthermore, the cross-linked polyplexes from IM-X with a fixed charge density exhibited even lower fluorescence intensity than the cross-linked MP polyplexes with a decreased charge density, showing that the additional disulfide cross-linking to the electrostatic interaction further promotes the condensation of pDNA.

Stability of Cross-Linked Systems. The stability of the cross-linked polyplexes against the counter polyanion exchange reaction may play a key role in pDNA release from the polyplexes in the intracellular compartment and was thus evaluated by the agarose gel electrophoresis as seen in Figure 5. The effects of cross-linking and charge densities on counter polyanion-induced dissociation of the polyplexes in nonreductive and reductive conditions were evaluated by this method. Obviously, in the nonreductive condition (Figure 5a, lane 2 and Figure 5b, lane 2), the bands of the free pDNA (super-coil and open-circular forms) were observed for the non-cross-linked systems (PEG-PLL and PDP-28 polyplexes). On the contrary, the free pDNA bands were not detected in the condition without DTT (Figure 5a, lanes 3 and 4 and Figure 5b, lanes 3−6) for all of the cross-linked systems (IM- and MP-polyplexes), indicating the substantial stabilization of the cross-linked polyplexes against the exchange reaction. Noteworthy is the behavior of MP-28 in the reductive medium containing 25 mM DTT (Figure 5b, lane 9): The free pDNA bands were only clearly observed for this system among all of the cross-linked polyplexes. This result indicates that the release of pDNA through the cleavage of the disulfide cross-linking occurs effectively with the polyplex designed to optimally balance the densities of charge and disulfide cross-linking.

In Vitro Transfection Efficiency of Cross-Linked Block Catiomer Polyplex. To assess the environmental sensitivity in the intracellular compartment, transfection of luciferase gene (pGL3) to cultured 293T cells was then carried out using these cross-linked polyplexes (Figure 6a). The cross-linked polyplexes of IM series, showing no release of entrapped pDNA in the electrophoretic assay under the reductive environment, resulted in an even lower transfection than the non-cross-linked control (PEG-PLL). This indicates that an additional introduction of disulfide cross-links to the polyplex with an appreciably high cationic charge density works synergistically to prevent pDNA release from the polyplex even in the reductive intracellular environment, resulting in a lowered transfection efficiency. Notably, the cross-linked polyplexes of MP series, the system compensating for the decrease in the charge density with the disulfide cross-linking, revealed an increased transfection efficiency compared to PEG-PLL, taking a maximum efficiency at MP-28 to achieve 1 order of magnitude higher luciferase expression than PEG-PLL. Note that this is reasonably consistent with their capability of pDNA release in the reductive environment as demonstrated in electrophoretic assay (Figure 5b). Progressive increase in gene expression with an increased thiolation degree up to 28% for MP series may be ascribed to the facilitated release of pDNA from the polyplex in the intracellular reductive environment due to the decreased charge density of ion-complexed polycation segment. On the other hand, MP-37 apparently revealed a lowered gene expression compared to MP-28. Release of pDNA from MP-37 is likely to be impeded even in the intracellular reductive environment, presumably due to the overstabilization through the excessive disulfide cross-linking. As seen in Figure 6b, PDP-28, the non-cross-linked control of MP-28, revealed only a 2 times higher transfection efficiency than PEG-PLL, indicating that the lowered charge density is not the main reason for the significantly higher efficiency of the MP-28 polyplex. It is reasonable to assume that disulfide cross-links may inhibit the MP-28

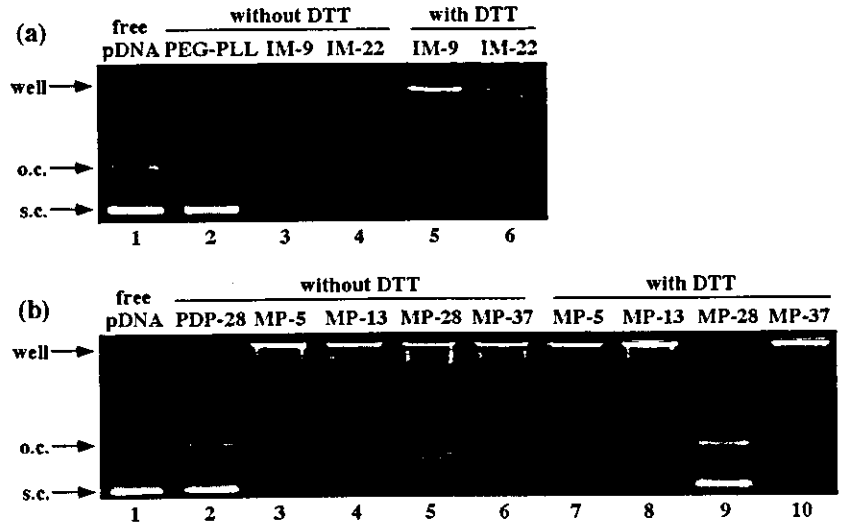

Figure 5. Agarose gel retardation analysis. Each sample was mixed with dextran sulfate (M_w = 25 000, ca. 20 times excess charge ratio to pDNA) and incubated at 37 °C for 24 h, followed by gel electrophoresis (final concentration of pDNA: 8.3 μg/mL). The reductive condition was prepared by adding DTT (25 mM). (a) Retardation assay for IM series. From left: lane 1, free pDNA; lane 2, PEG-PLL polyplex; lanes 3 and 4, IM-X polyplex without DTT; lanes 5 and 6, IM-X polyplexes with 25 mM DTT. (b) Retardation assay for MP series. From left: lane 1, fee pDNA; lane 2, PDP-28; lanes 3–6, MP-X without DTT; lanes 7–10, MP-X with 25 mM DTT. (s.c., supercoiled; o.c., open circular form of pDNA).

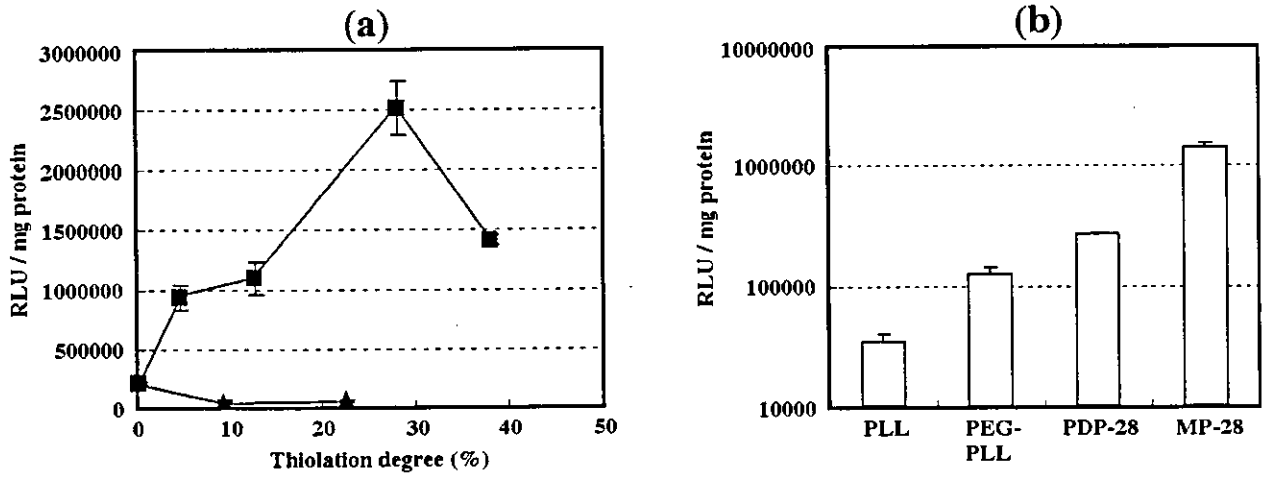

Figure 6. Transfection of luciferase gene to 293T cells by the block catiomer polyplexes. 293T cells were incubated with the polyplexes in the medium containing 100 μM hydroxychloroquine (HC) and 10% serum for 24 h, followed by an additional 24 h culture without the polyplexes and HC in the medium containing 10% serum. (a) Effect of the thiolation degree on the transfection efficiency. (■) MP-X polyplex, (▲) IM-X polyplex. (b) Progressive increase in transfection with a modulation in the structure of PLL-based polyplexes. PLL (poly(L-lysine) homopolymer, M_w = 18 000) was used as the control polyplex.

polyplex from disintegrating in the extracytoplasmic environment, allowing the effective intracellular delivery of pDNA. Subsequently, the cleavage of the disulfide bond in the reductive intracellular compartment triggers the efficient release of pDNA from the MP-28 polyplex, because it should induce a substantial decrease in the association force in the polyplex, a system compensating the decreased charge with disulfide cross-linking.

From a practical viewpoint, long-term storage of gene carriers in a regulatory condition, including powdered and frozen formulations, is a crucial issue. Nevertheless, the conventional lipoplexes and polyplexes are not tolerant of freezing, resulting in a significant loss in the transfection efficiency in the absence of particular saccharide compounds as lyoprotectants.[19–21] As seen in Figure 7, the disulfide cross-linking (MP-28) completely protects the transfection capacity of the block catiomer polyplexes even after the simple freeze–thawing without using any protective reagents. This is in a sharp contrast to the significantly lowered transfection efficiency of non-cross-linked polyplexes after the freeze–thawing process. The disulfide cross-linking obviously prevents the polyplex from the structural change induced by freezing stress. Indeed, there was no substantial change in AFM images of the cross-linked polyplexes before and after the freeze–thawing process (data not shown).

Conclusions

Here, the disulfide cross-linked polyplex is shown to undergo the environment-sensitive release of pDNA through the regulated

(19) Talsma, H.; Cherng, J.-Y.; Lehrmann, H.; Kursa, M.; Ogris, M.; Hennink, W. E.; Cotten, M.; Wagner, E. *Int. J. Pharm.* **1997**, *157*, 233–238.
(20) Cherng, J.-Y.; Wetering, P.; Talsma, H.; Crommelin, D. J. A.; Hennink, W. E. *Pharm. Res.* **1997**, *14*, 1838–1841.
(21) Anchordoquy, T. J.; Carpenter, J. F.; Kroll, D. J. *Arch. Biochem. Biophys.* **1997**, *348*, 199–206.

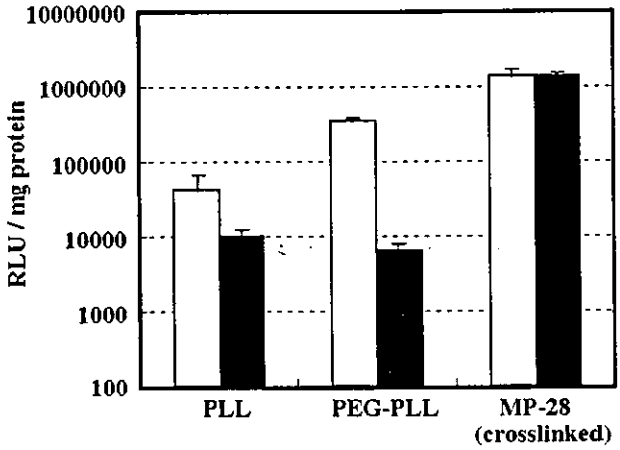

Figure 7. Effect of freeze−thawing on the transfection efficiency of polyplexes. Open bar: nonfrozen sample. Closed bar: freeze−thawed sample. All the polyplex samples were frozen at −20 °C for 2 h, followed by thawing at room temperature for 30 min. PLL represents poly(L-lysine) homopolymer (M_w = 18 000).

cleavage of disulfide bond in the reductive condition. The cross-linked polyplexes with a lowered charge density (MP-X polyplexes), in particular MP-28, achieved significantly higher transfection than those with a fixed charge density (IM-X polyplexes). The presence of the optimal thiolation degree (28%) in MP-X supports our hypothesis that the efficient transfection in the disulfide cross-linked polyplexes can be achieved by controlling the balance between the cationic charge and disulfide cross-linking densities. Our results should provide a comprehensive knowledge of designing the environment-sensitive polyplex systems with high stability in extracellular environments and an effective releasing capacity of pDNA in intracellular compartments for the efficient transfection. Our recent animal study revealed an appreciable gene expression in mouse liver for intravenously injected MP-28, and detailed results will be reported elsewhere in near future.

Acknowledgment. This work was financially supported by the Core Research Program for Evolutional Science and Technology (CREST) from the Japan Science and Technology Corporation (JST) as well as by Special Coordination Funds for Promoting Science and Technology from the Ministry of Education, Culture, Sports, Science and Technology of Japan (MEXT). We express our appreciation to Mr. Hiroshi Nagano, The University of Tokyo, and Mr. Shigeto Fukushima, Nippon Kayaku Co., Ltd., Japan, for their help with the polymer synthesis.

JA0379666

VOLUME 22 NUMBER 3 MARCH 2004
www.nature.com/naturebiotechnology

nature biotechnology

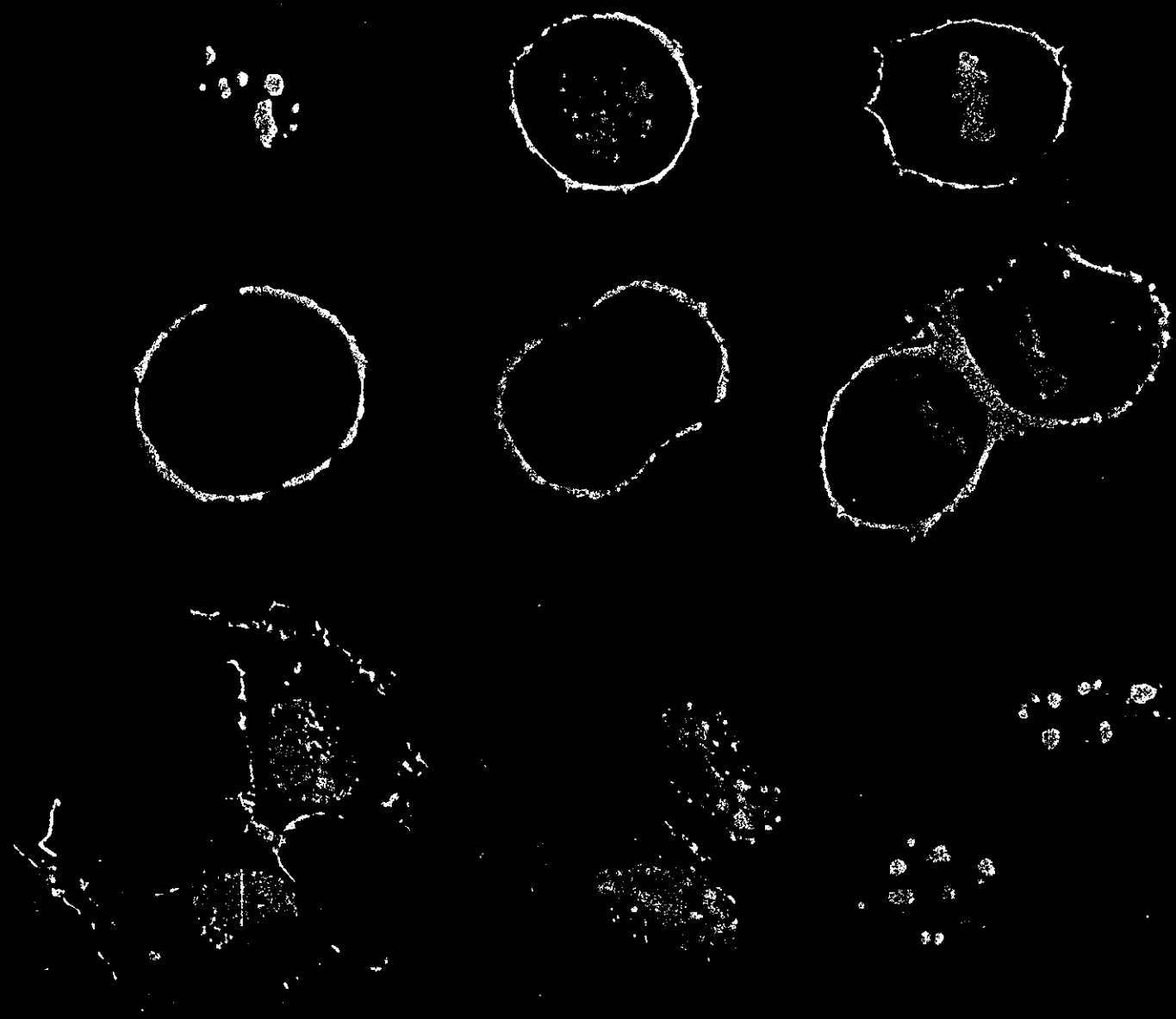

Watching the clock in mitosis

Circumventing siRNA interferon induction

Immortalized neural progenitors

nature
biotechnology

Nanospheres for DNA separation chips

Mari Tabuchi[1,5,6], Masanori Ueda[1,5], Noritada Kaji[1,5], Yuichi Yamasaki[2,5], Yukio Nagasaki[3,5], Kenichi Yoshikawa[4,5], Kazunori Kataoka[2,5] & Yoshinobu Baba[1,5,6,7]

We report here a technology to carry out separations of a wide range of DNA fragments with high speed and high resolution. The approach uses a nanoparticle medium, core-shell type nanospheres, in conjunction with a pressurization technique during microchip electrophoresis. DNA fragments up to 15 kilobase pairs (kbp) were successfully analyzed within 100 s without observing any saturation in migration rates. DNA fragments migrate in the medium while maintaining their characteristic molecular structure. To guarantee effective DNA loading and electrofocusing in the nanosphere solution, we developed a double pressurization technique. Optimal pressure conditions and concentrations of packed nanospheres are critical to achieve improved DNA separations.

Genome projects are accomplished using DNA sequencing systems based on capillary array electrophoresis. However, more powerful and simple analytical systems for separation of biopolymers (DNA fragments and proteins) will be required to rapidly and precisely analyze samples. Although microchip electrophoresis techniques combined with hydrophilic polymer media appear to be promising, particularly for some DNA separations[1,2], the separation of longer DNAs (greater than several kbp) still results in electrophoretic mobility that is independent of length in conventionally available media[3]. Consequently, estimation of DNA size in these systems is ambiguous. In addition, high-viscosity polymer solutions are usually used in these experiments to obtain good resolution, and the handling of these types of solutions can be difficult. Several low-viscosity media[4–10] and various techniques using nanofluidic[11–14] or magnetic[15] structures have been developed to improve biopolymer size separation methodologies.

These methods have led to significant advances in separation technology, such as a poly(dimethylacrylamide) (POP-6^T)[4] for DNA sequencing, and some of them will find practical use in functional genome and proteome projects and clinical applications in the near future. However, these systems are applicable only for separations within a limited size range (less than 1 kbp[4,9] or greater than several kbp[7,8,10–15]) and they require thermo-control[5,6] or other expensive and robust devices[11–15]. Here we describe an effective and simple analytical system based on core-shell type nanosphere technology, which is applicable to separation of DNA fragments across a broad size range.

We recently developed a core-shell type of globular nanoparticle (nanosphere) which was prepared by the multimolecular micellization and subsequent core polymerization of block copolymer of poly(ethylene glycol) with poly(lactic acid) possessing a methacryloyl group at the PLA chain end (PEG_m-β-PLA_n-MA_l; Mw(PEG/PLA) = 6,100/4,000, m ≈ 100, n ≈ 40, l ≈ 70) in aqueous medium[16]. The hydrophobic PLA segments form a spherical core, which is covered by tethered, flexible PEG chains at a fairly high density. The methacryloyl groups located in the particle core were polymerized to form stable core-shell type nanospheres having a diameter of 30 nm (Fig. 1a). The nanospheres have no surface charge, and they have a narrow size distribution and low viscosity in aqueous media (0.94 cP at 1.0% (10 mg/ml)) compared with conventional polymers (*e.g.*, methylcellulose: 8.8 cP at 0.5% and 104 cP at 1.0%), owing to their globular structure. We anticipate that these nanoparticles will provide a suitable nano-packing medium for use as a sieving matrix in microchannels. Our calculations show that the nanospheres form a close-packed structure at 1% concentration. Our hypothesis was that densely packed nanospheres with PEG-tethered chains on their surface would improve both the handling properties and the separation of DNA samples, thus providing a method potentially applicable to several high-throughput technologies.

To attain high-speed and improved resolution, we developed a double pressurization technique as an essential component of this nanosphere system. After filling all channels in a microchip with a 1% nanosphere solution, the sample was injected from the vertical direction by initial pressure (P_{1st}) application (P_{1st} = 2.5 kPa for 1 s; Fig. 1b, left (i)). Each sample was introduced to the cross section. Just before electrophoretic separation, a secondary pressure (P_{2nd}) was applied for 1 s to the separation channel (P_{2nd} = 2.5 kPa for 1s; Fig. 1b, left (ii)), causing the sample at the cross section to advance further as a dispersed broad band without electric field. Subsequently, electrophoresis was done at 220 V/cm (Fig. 1b, left (iii) for 0.5 s and (iv) for 1 s) without pressure. The sample band, which initially showed a broad parabolic flow after the P_{2nd} application, was focused by this electrophoretic process to form a plug flow (Fig. 1b, left (iii) and (iv)).

[1]Department of Medicinal Chemistry, Faculty of Pharmaceutical Sciences, The University of Tokushima, 1-78 Shomachi, Tokushima 770-8505, Japan. [2]Department of Material Science, Graduate School of Engineering, The University of Tokyo, 7-3-1 Hongo, Bunkyo-ku, Tokyo 113-8656, Japan. [3]Department of Materials Science and Technology, Tokyo University of Science, Noda 278-8510, Japan. [4]Department of Physics, Graduate School of Science, Kyoto University, Kyoto 606-8502, Japan. [5]CREST, Japan Science and Technology Agency, JST, Japan. [6]The 21st Century COE Program, Human Nutritional Science on Stress Control, The University of Tokushima, Tokushima, Japan. [7]Single-molecule Bioanalysis Laboratory, National Institute of Advanced Industrial Science and Technology, AIST, Hayashi-cho 2217-14, Takamatsu, 761-0395, Japan. Correspondence should be addressed to M.T. (tabuchi@ph.tokushima-u.ac.jp).

Published online 8 February 2003; doi:10.1038/nbt939

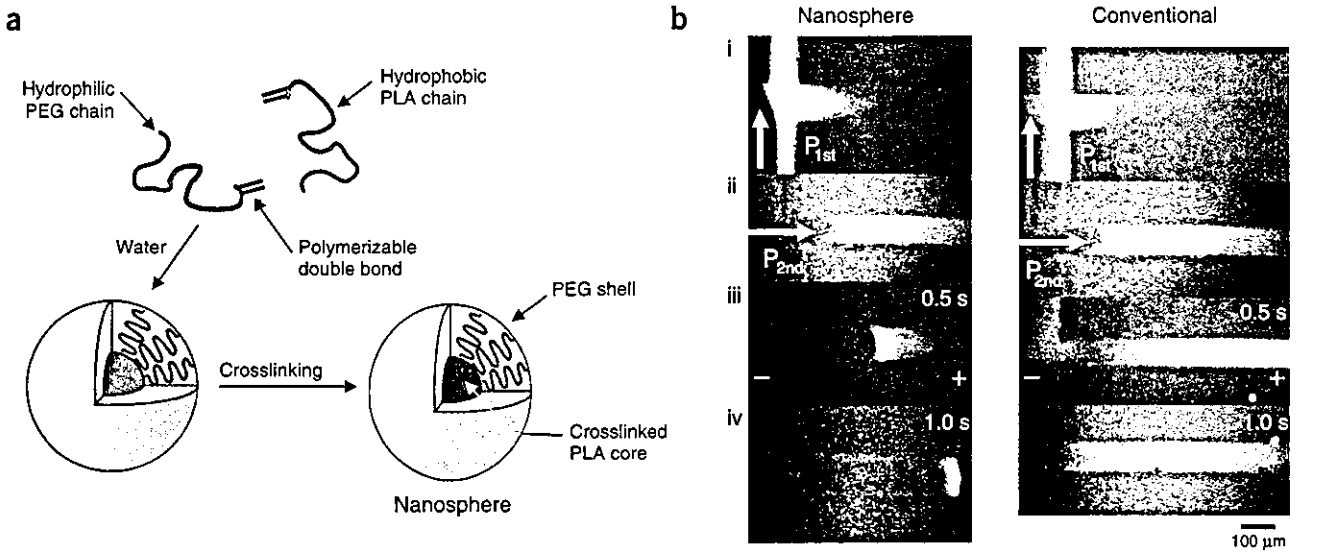

Figure 1 The new system using nanospheres and a double pressurization technique. (**a**) Images of the core-shell type nanosphere structure (nanosphere). (**b**) Fluorescence images taken during application of the double pressurization technique. We observed the sample plug formation (20 ng/μL of 200 bp DNA from Genesura Laboratories with 0.8 μM of the fluorescent dye YOYO1 (Molecular Probes) in 4% 2-mercaptoethanol in TE buffer). Arrows show the pressure application. The horizontal channel is a separation channel. (i) P_{1st}: 2.5 kPa, 1s; after filling all channels with solution (1% nanosphere solution (left), 0.5% methylcellulose (right)) the sample was injected by P_{1st} for 1 s using a syringe from the bottom well of the loading channel, with the top and right wells open. (ii) P_{2nd}: 2.5 kPa, 1s; the sample band introduced into the cross section was advanced by P_{2nd} for 1 s from the left well and in the right direction with the top and bottom wells open. (This places the sample between the layers of the nanospheres (left).) (iii) Electrophoretic separation: 160 V/cm, 0.5 s. (iv) Electrophoretic separation: 160 V/cm, 1 s.

The usual electrokinetic injection of samples without pressurization onto the nanosphere solutions could not generate a sufficiently intense band and no peaks appeared (data not shown). When the same pressurization technique was applied to the conventional polymer solution, the focusing of the broad band did not occur (Fig. 1b, right). The electrofocusing, which was observed only in the nanosphere system, seems to be a stacking effect of the packed nanospheres.

Figure 2a shows an electropherogram of DNA fragments generated using both conventional media and nanospheres. High-speed separation of DNA fragments was attained using nanospheres (60 s in nanosphere medium versus 130 s in conventional polymer medium for 100–1,000 bp (Fig. 2a, left) and 100 s in nanosphere medium versus 200 s in conventional polymer medium for a 1–15 kbp DNA ladder (Fig. 2a, right)). The DNA strands whose mobility is independent of length in conventional polymer solutions (800–1,000 bp for a 100–1,000 bp DNA ladder (Fig. 2a, left) and 6–15 kbp for a 1–15 kbp DNA ladder (Fig. 2a, right)) were successfully eliminated by the nanospheres. A wide range of DNA fragments between 1 and 15 kbp was successfully analyzed within 100 s without observing any saturation in migration rates.

All peaks over a wide range of DNA fragment sizes (1–15 kbp) were separated by adjusting the initial pressure conditions (P_{1st}: 10 kPa for 1 s, Fig. 2a (top right)). As the P_{2nd} was increased from 1 kPa to 10 kPa, the migration time decreased while resolution was retained (for 100 bp double-stranded DNA (dsDNA) ladder: 1 kPa within 150 s; 5 kPa, 90 s; and 10 kPa, 60 s; and for 1 kbp dsDNA ladder: 1 kPa within 180 s; 5 kPa, 140 s; and 10 kPa, 100 s). This suggests that the migration time is dependent upon the degree of pressurization, which may result in a shortened overall effective channel length. However, when a commercially available polymer solution was used, application of P_{2nd} above 2.5 kPa produced broad peaks and the resolution was reduced.

The log-log plots of the relative mobility versus DNA fragment size[17] show that the 'nanospheres with pressurization' method is clearly different from conventional methods (Fig. 2b). A prolonged inverse proportional relationship was observed (Fig. 2b, [▲]), whereas routine methods using a conventional polymer resulted in a plateau of size-based mobility (Fig. 2b, [○]). There was no plateau region (that is, region of 'length-independent electrophoretic mobility') in the range of DNA sizes measured in this study for nanospheres with pressurization. Although some techniques using ultra-diluted polymer solutions and end-labeled free solution electrophoresis methods have produced improvements in migration decay (loss of resolution)[7,9], it is impossible to accurately analyze a broad range of DNA fragment sizes using these methods. The nanosphere and pressurization technique now makes it possible to analyze a broader range of DNA fragment sizes without compromising either the time required for analysis or the migration saturation.

To further analyze the differences in DNA migration in nanosphere solutions versus conventional gels, we visualized the migration of a single DNA molecule directly by fluorescence microscopy (Fig. 3). Surprisingly, under an electric field the segregated DNA molecules maintained a 'relaxed' conformation with minimal stretching motion in the nanosphere solution (Fig. 3a), in contrast to the usual behavior of DNA in a conventional gel, which involves repetitive stretching and contraction (Fig. 3b). Usually, long fragments of DNA in conventional matrices (gels or polymers) align in the direction of the electric field and migrate headfirst, showing an I- or U-shaped DNA structure, which will always involve some stretching[18–20].

The characteristic behavior of DNA in nanospheres indicates that the mechanism of long DNA separation is fundamentally different from traditional mechanisms (Fig. 3a). The DNA molecules exhibit intrachain segregation[21], where folded compact regions (mini-globules) and unfolded coil regions coexist within a single DNA (Fig. 3a,

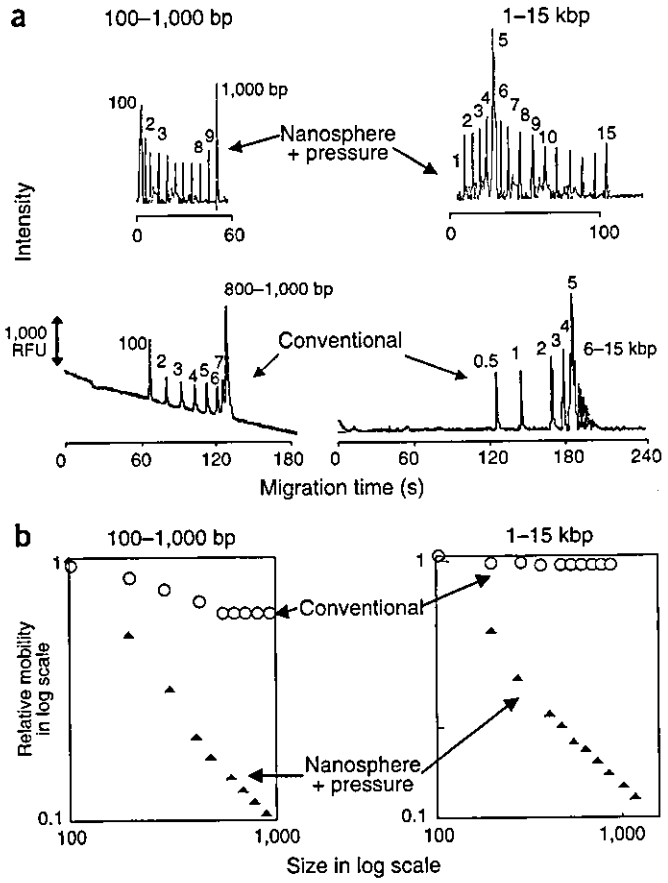

Figure 2 Effectiveness of DNA separations carried out using conventional polymers versus nanospheres with pressurization methods. (**a**) Electropherograms are shown for the following samples. A 1 μg/ml solution of a 100 bp dsDNA ladder containing 10 fragments (Nonagen; 100–1,000 bp; the 100 and 1,000 bp bands are strong) in a 1% (10 mg/ml) nanosphere solution, pH 9, P_{1st}: 2.5 kPa and P_{2nd}: 2.5 kPa (upper left). A 1 μg/mL solution of a 1 kbp dsDNA ladder containing 15 fragments (Nonagen; 1–15 kbp; the 5 kbp band is strong) in a 1% (10 mg/mL) nanosphere solution, pH 9, P_{1st}: 10 kPa and P_{2nd}: 10 kPa (upper right). The 100 bp dsDNA ladder in a conventional polymer (0.5% methylcellulose) solution using conventional electrophoresis (lower left). The 1 kbp dsDNA ladder in a conventional polymer (0.5% methylcellulose) solution using conventional electrophoresis (lower right). (**b**) Log-log plots of the relative mobility versus DNA fragment size. The 100–1,000 bp dsDNA ladder (left), the 1–15 kbp dsDNA ladder (right) for the conventional polymer using conventional electrophoresis [O] and the nanosphere solution with double pressurization method [▲]. RFU, relative fluorescent units.

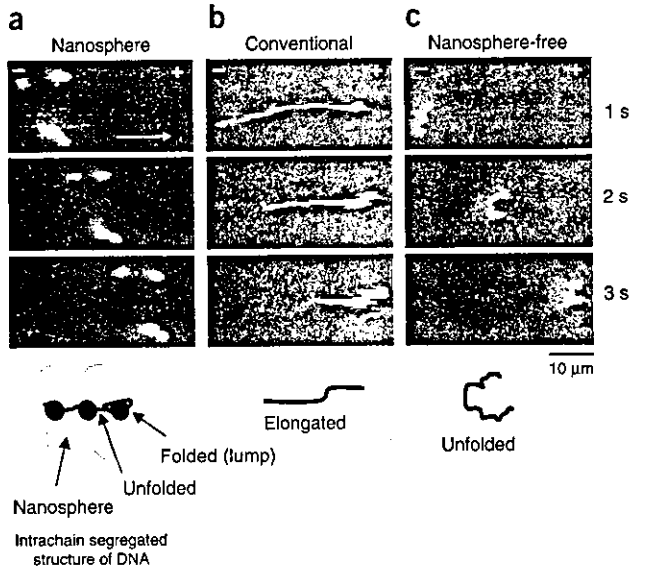

Figure 3 Visualization of single DNA molecules. (**a**,**b**) Sequential fluorescent images of DNA migration behavior (T4 DNA, 165.6 kbp, Takara Bio) under an electric field (10 V) in a 1% nanosphere solution (**a**), a conventional agarose gel (**b**) (1% agarose NA (Amersham Pharmacia Biotech AB), and a control buffer containing no nanospheres (**c**). An illustration of typical DNA conformation is given at the bottom of each figure.

bottom). Note that this intrachain segregated structure also appears in the nanosphere solutions without an electric field, but does not appear in a nanosphere-free solution with (Fig. 3c) or without the electric field, indicating that the nanosphere matrix itself provides the environment required to induce this phenomenon. Because the close-packed structure of nanospheres includes dense regions and a limited amount of extra space, the unfolded coil structure was seen along with regular lumps of DNA (Fig. 3a, bottom). The stretching of DNA is minimal in the nanosphere solution, a consequence of the confined environment, even under an electric field. As a result, DNA molecules migrate while maintaining an intrachain segregated structure within the nanospace. However, to attain such separations, it was necessary to work out optimized conditions for the nanosphere solution. For example, a dilute solution of nanospheres (<1%), in which wider spaces exist between nanospheres, did not produce adequate separations. An effective nanospace is produced by optimizing the concentration of packed nanospheres, which is critical to achieve improved DNA separations. Under optimal packing conditions, physical interaction between the lumps of DNA and the nanospheres might occur, an interaction that may be responsible for the size separation observed. However, a theoretical explanation for the separation method described here has not yet been obtained.

Besides the characteristic intrachain segregated structure seen in nanospheres, the pressurization technique also seems to have contributed to the improved DNA separation, given that both a nanosphere medium and precisely controlled pressurization were needed for the system to work (Fig. 1b). A double pressurization technique was specially developed for microchip electrophoresis using nanospheres. When the P_{1st} and/or P_{2nd} pressurization were not applied, the separation was impossible or was inadequate. The pressurization technique with the nanospheres is the methodology that leads to effective DNA loading, electrofocusing and a shortened effective channel length (Fig. 1b). In addition, adjustment of the pressure force enabled the separation of a wide range of DNA fragments without saturation of migration rates (Fig. 2a). This seems to indicate that nanospaces between nanospheres can be optimized by the pressurization technique. Therefore, the pressurization technique is an essential component of this nanosphere system methodology.

In conclusion, the nanosphere system described here readily separates DNA fragments over a wide range of sizes with higher speed than conventional methods. To use the nanospheres for microchip electrophoresis, samples have to be introduced initially under pressure. Before electrophoretic separation, a secondary application of pressure to the nanospheres accelerates the separation speed of the DNA. The introduced DNA fragments migrate and became focused within the nanosphere solutions under an electric field. The characteristic

'lumps' of DNA intrachain segregated structures are generated in a specific environment of condensed nanospheres. This technology should find wide use in high-throughput analytical systems, including medical diagnoses involving biopolymer analysis. The low viscosity, effective, core-shell type nanosphere method is fully competitive with, and in many cases superior to, conventional separation techniques currently used for analysis of DNA and other biopolymers.

METHODS

Microchip electrophoresis conditions. A microchip electrophoresis system (SV1100 Hitachi Electronics Engineering) and a microchip (i-chip 3; Hitachi Chemical), made of poly(methyl methacrylate) with channels 100 μm wide and 30 μm deep, and a 30 mm effective separation channel were used. In conventional separations, after samples were loaded by voltage (300 V), a separation voltage (890 V) was applied to the separation channel and a squeezing voltage (130 V) was applied to the cross section. The electrophoresis was done at 25 °C. For the new method, after filling all channels on a microchip with a 1% nanosphere solution, the sample was placed at the sample well and was injected into the channels by a P_{1st} application (1–10 kPa for 1s) using a syringe, with the opposite and outlet wells open. Just before electrophoretic separation, P_{2nd} (1–10 kPa for 1 s) was applied to the separation channel from the inlet without an electric field. Subsequently, electrophoresis was done at 220 V/cm with a squeezing voltage of 130 V without pressure (**Supplementary Methods** and **Supplementary Fig. 1** online).

Direct observation of a migrating single DNA. An inverted fluorescence microscope (Axiovert 135TV, Carl Zeiss) was used for direct observation of a single migrating DNA molecule, and fluorescence images were taken to illustrate the results of the various injection modes. Electric fields generated by a multifunction synthesizer (1942, NF Corp.) were applied between the two platinum electrodes through a high-speed power amplifier bipolar power supply (4020, NF CORPORATION). A HVS448 High Voltage Sequencer, LabSmith (HVS448 High Voltage Sequencer) was used to analyze the injection modes.

Note: Supplementary information is available on the Nature Biotechnology website.

ACKNOWLEDGMENTS

This work was partially supported by a grant funding Core Research for Evolutionary Science and Technology from the Japan Science and Technology Agency, a grant from the New Energy and Industrial Technology Development Organization of the Ministry of Economy, Trade and Industry, Japan, a Grant-in-Aid for Scientific Research from the Ministry of Education, Science and Technology, Japan, and the 21st Century COE Program, Human Nutritional Science on Stress Control, Tokushima, Japan. We thank Chie Kuwahara, Ryosuke Kodaka and Fumiko Aboshi of the Tokyo University of Science and Eduardo Jule of the University of Tokyo for preparing the nanospheres. The authors would like to thank Tomoaki Hino, Ken Hirano, Fung Xu, Mohammad Jabasini, Hideya Nagata, Yasuko Tanaka and Emi Endo of the University of Tokushima for technical and secretarial assistance.

COMPETING INTERESTS STATEMENT

The authors declare that they have no competing financial interests.

Received 21 October; accepted 24 November 2003
Published online at http://www.nature.com/naturebiotechnology/

1. Wehr, T., Zhu, M. & Mao, D.T. in *Capillary Electrophoresis of Nucleic Acid*, vol. I (eds. Mitchelson, K.R. & Cheng, J.) 167–187 (Humana Press, Totowa, NJ, 2001).
2. Viovy, J.L. & Duke, T. DNA electrophoresis in polymer solutions: ogston sieving, reptation and constraint release. *Electrophoresis* **14**, 322–329 (1993).
3. Slater, G.W., Desruisseaux, C. & Hubert, S.J. in *Capillary Electrophoresis of Nucleic Acid*, vol. I (eds. Mitchelson, K.R. & Cheng, J.) 27–34 (Humana Press, Totowa, NJ, 2001).
4. Madabhushi, R.S. Separation of 4-color DNA sequencing extension products in noncovalently coated capillaries using low viscosity polymer solutions. *Electrophoresis* **19**, 224–230 (1998).
5. Lie, Y. & Rill, R.L. in *Capillary Electrophoresis of Nucleic Acid*, vol. I (eds. Mitchelson, K.R. & Cheng, J.) 203–213 (Humana Press, Totowa, NJ, 2001).
6. Buchholz, B.A. *et al.* Microchannel DNA sequencing matrics with a thermally controlled "Viscosity switch." *Anal. Chem.* **73**, 157–164 (2001).
7. Barron, A.E., Blanch, H.W. & Soane, D.S. A transient entanglement coupling mechanism for DNA separation by capillary electrophoresis in ultradilute polymer solution. *Electrophoresis* **15**, 597–615 (1994).
8. Hubert, S.J., Slater, G.W. & Viovy, J.-L. Theory of capillary electrophoretic separation of DNA using ultradilute polymer solution. *Macromolecules* **29**, 1006–1009 (1996).
9. Heller, C. *et al.* Free-solution electrophoresis of DNA. *J. Chromatography A* **806**, 113–121 (1998).
10. Ren, H. *et al.* Separation DNA sequencing fragments without a sieving matrix. *Electrophoresis* **20**, 2501–2509 (1999).
11. Volkmuth, W.D. & Austin, R.H. DNA electrophoresis in microlithography arrays. *Nature* **358**, 600–602 (1992).
12. Chou, C.-F. *et al.* Sorting by diffusion: an asymmetric obstacle course for continuous molecular separation. *Proc. Natl. Acad. Sci. USA* **23**, 13762–13765 (1999).
13. Han, J. & Craighead, H.G. Separation of long DNA molecules in a microfabricated entropic trap array. *Science* **288**, 1026–1029 (2000).
14. Hung, L.R. *et al.* A DNA prism for high-speed continuous fractionation of large DNA molecules. *Nat. Biotechnol.* **20**, 1048–1051 (2002).
15. Doyle, P.S., Bibette, J., Bancaud, A. & Viovy, J.-L. Self-assembled magnetic matrices for DNA separation chips. *Science* **295**, 2237 (2002).
16. Iijima, M., Nagasaki, Y., Okada, T., Kato, M. & Kataoka, K. Core-polymerized reactive micelles from heterotelechelic amphiphilic block copolymers. *Macromolecules* **32**, 1140–1146 (1999).
17. de Gennes, P.G. Reptation of a polymer chain in the presence of fixed obstacles. *J. Chem. Phys.* **55**, 572–579 (1971).
18. Schwartz, D.C. & Koval, M. Conformational dynamics of individual DNA molecules during gel electrophoresis. *Nature* **338**, 520–522 (1989).
19. Smith, S.B., Aldridge, P.K. & Callis, J.B. Observation of individual DNA molecules undergoing gel electrophoresis. *Science* **243**, 203–206 (1989).
20. Shi, X., Richard, R.W. & Morris, M.D. DNA conformational dynamics in polymer solutions above and below the entanglement limit. *Anal. Chem.* **67**, 1132–1138 (1995).
21. Yoshikawa, K. Controlling the higher-order structure of giant DNA molecules. *Adv. Drug Del. Rev.* **52**, 235–244 (2001).

FEBS 27897

FEBS Letters 557 (2004) 21–25

Effective accumulation of polyion complex micelle to experimental choroidal neovascularization in rats

Ryuichi Ideta[a,1], Yasuo Yanagi[a,*], Yasuhiro Tamaki[a], Fumitaka Tasaka[a,b,1], Atsushi Harada[c], Kazunori Kataoka[d]

[a]*Department of Ophthalmology, University of Tokyo School of Medicine, 7-3-1 Hongo, Bunkyo-ku, Tokyo 113-8655, Japan*
[b]*Research and Development Division, Santen Pharmaceutical Co., Ltd., 8916-16 Takayama-cho, Ikoma, Nara 630-0101, Japan*
[c]*Department of Applied Materials Science, Graduate School of Engineering, Osaka Prefecture University, 1-1 Gakuen-cho, Sakai, Osaka 599-8531, Japan*
[d]*Department of Materials Science and Engineering, Graduate School of Engineering, The University of Tokyo, 7-3-1 Hongo, Bunkyo-ku, Tokyo 113-8656, Japan*

Received 26 September 2003; revised 6 November 2003; accepted 7 November 2003

First published online 22 December 2003

Edited by Guido Tettamanti

Abstract **Exudative age-related macular degeneration, characterized by choroidal neovascularization (CNV), is a major cause of visual loss. In this study, we examined the distribution of the polyion complex (PIC) micelle encapsulating FITC-P(Lys) in blood and in experimental CNV in rats to investigate whether PIC micelle can be used for treatment of CNV. We demonstrate that PIC micelle has long-circulating characteristics, accumulating to the CNV lesions and is retained in the lesion for as long as 168 h after intravenous administration. These results raise the possibility that PIC micelles can be used for achieving effective drug targeting to CNV.**

Key words: Age-related macular degeneration; Choroidal neovascularization; Drug delivery system; Nanotechnology; Polyion complex micelle

1. Introduction

Exudative age-related macular degeneration (AMD), characterized by choroidal neovascularization (CNV), is a major cause of visual loss in developed countries [1,2]. Photocoagulation of the entire CNV is an effective treatment option for exudative AMD proved in large randomized control studies performed by the Macular Photocoagulation Study Group [3]. However, since most CNV extends to the subfovea, permanent central visual loss is inevitable immediately after photocoagulation. Thus, alternative treatments for CNV with minimal damage to the healthy retina, such as photodynamic therapy, are being developed [4]. In addition, compounds with anti-angiogenic properties are under intensive study for possible clinical applications [5,6]. Although studies in vivo using animal CNV models have demonstrated the favorable results of several anti-angiogenic drugs such as interferon-β and thalidomide, these drugs were not effective in inhibiting the development of CNV in humans. To develop a pharmacological therapy for CNV with minimal systemic adverse effects, it is necessary to achieve a high local concentration of the drug [7].

These results have prompted the search for an alternative drug delivery system. Macromolecules can accumulate and prolong their retention in perivascular regions of solid tumors to a greater extent than in normal tissues because newly formed vessels in solid tumors exhibit high substance permeability compared with those in normal tissues, and the lymph systems in tumor tissue are incomplete [8,9]. This effect is known as the enhanced permeability retention (EPR) effect [10]. CNV membranes have high permeability and several studies have demonstrated that macromolecules accumulate in experimental CNV presumably through the EPR effect [7].

The size of the molecules is an important factor in exerting the EPR effect. Polymeric micelles have a size range of several tens of nanometers with a very narrow distribution, similar to that of viruses and lipoproteins [8]. Thus, they accumulate in solid tumors through the EPR effect [11,12]. In addition, compared with the drug delivery system based on macromolecule conjugates, polymeric micelle can stably encapsulate chemical compounds with high efficiency [8]. On the basis on this together with their high drug-loading capacity, polymeric micelles are expected to become a novel drug delivery system. In fact, we have developed a drug delivery system with polymeric micelles encapsulating doxorubicin [13] and it is now in phase II clinical trial for the treatment of solid tumors [14].

We have recently developed a novel type of polymeric micelle formed through electrostatic interaction (polyion complex (PIC) micelle) [8,15]. Unlike polyion complexes formed from an oppositely charged pair of simple homopolymers or statistical copolymers, PIC micelles from charged block copolymers are totally water-soluble and are narrowly distributed. In this study, to investigate whether PIC micelle can be used for treatment of CNV, we examined the distribution of the PIC micelle in blood and in experimental CNV in rats.

*Corresponding author. Fax: (81)-3-3817 0798.
E-mail address: yanagi-tky@umin.ac.jp (Y. Yanagi).

[1] These authors contributed equally to this work.

Abbreviations: AMD, age-related macular degeneration; CNV, choroidal neovascularization; DLS, dynamic light scattering; EPR, enhanced permeability retention; PIC, polyion complex

0014-5793/03/$30.00
doi:10.1016/S0014-5793(03)01315-2

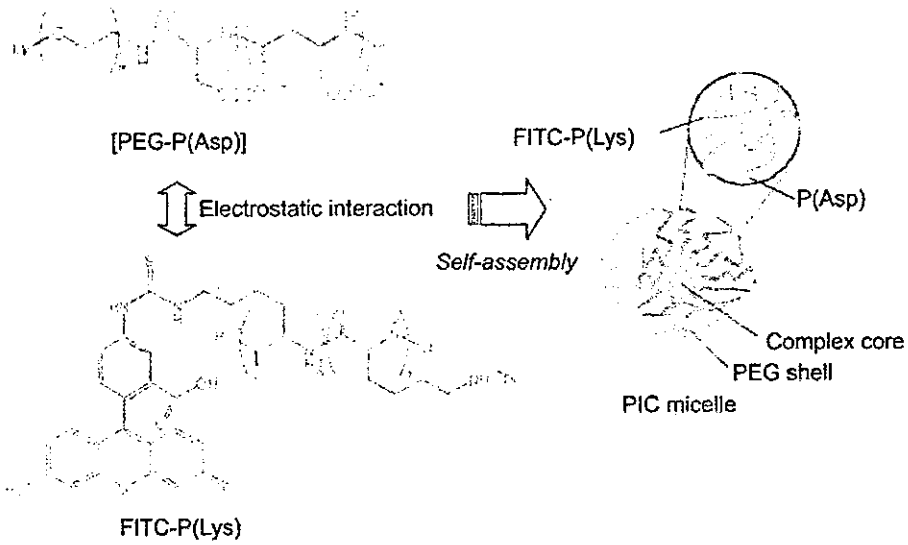

Fig. 1. Preparation and schematic structure of PIC micelle encapsulating FITC-P(Lys). PIC micelle consists of an inner complex core formed by the P(Asp) segment and FITC-P(Lys), and an outer PEG shell.

2. Materials and methods

2.1. Animals

Male Brown Norway rats weighing 100–120 g were obtained from Saitama Animal Lab (Saitama, Japan). All experiments were conducted in accordance with the Animal Care and Use Committee and the Association for Research in Vision and Ophthalmology Statement for the Use of Animals in Ophthalmic and Vision Research.

2.2. Experimental CNV

A general anesthesia was induced with an intraperitoneal injection (1000 μl/kg) of a mixture (7:1) of ketamine hydrochloride (Ketalar®, Sankyo, Tokyo, Japan) and xylazine hydrochloride (Celactal®, Bayer, Tokyo, Japan) or by inhalation of diethyl ether. The pupil was dilated with one drop of 0.5% tropicamide (Mydrin® M, Santen Pharmaceutical, Osaka, Japan) for photocoagulation. Experimental CNV was created as previously described [16,17]. Fifty laser photocoagulations were applied to each eye between the major retinal vessels around the optic disc with a diode laser photocoagulator (DC-3000®, Nidek, Osaka, Japan) and a slit lamp delivery system (SL150, Topcon, Tokyo, Japan) at a spot size of 75 μm, duration of 0.05 s, and intensity of 200 mW.

2.3. Preparation of PIC micelle encapsulating fluorescein isothiocyanate-labeled poly-L-lysine (Fig. 1)

Fluorescein isothiocyanate-labeled poly-L-lysine [FITC-P(Lys), 100.0 mg; polymerization degree = 105, FITC = 0.004 mol/mol of Lys] and 48.6 mg of polyethylene glycol-*block*-poly-α,β-aspartic acid) [PEG-P(Asp); PEG MW = 5000 g/mol, polymerization degree of P(Asp) segment = 78] were dissolved in 10.0 and 5.0 ml of phosphate-buffered saline (PBS), respectively. PIC micelle solution was prepared by mixing the same volume (5.0 ml) of FITC-P(Lys) and PEG-P(Asp) solutions, in which the molar ratio of Lys and Asp residues was adjusted to unity. As a control, 5.0 ml of FITC-P(Lys) solution was diluted in 5.0 ml of PBS. Both PIC micelle and control solutions included the same concentration (5.0 mg/ml) of FITC-P(Lys). The average diameter and polydispersity index of PIC micelles was evaluated by dynamic light scattering (DLS) measured at 25°C, using a light scattering spectrophotometer (DLS-7000, Otsuka Electronics, Osaka, Japan) with a vertically polarized incident beam at 632.8 nm supplied by a He/Ne laser. A scattering angle of 90° was used in this study.

2.4. Accumulation of PIC micelle to CNV lesions: histological analysis

To investigate the accumulation of PIC micelle to the CNV lesions, 50 photocoagulations were applied to the right eye of a total of 23 rats. The left eyes served as non-photocoagulation controls. By tail injection, 400 μl of PIC micelle encapsulating 5.0 mg/ml FITC-P(Lys) or 400 μl of free FITC-P(Lys) at a concentration of 5.0 mg/ml ($n = 3$) was administered to rats 7 days after photocoagulation. There was high mortality in rats receiving FITC-P(Lys) after 1 h, suggesting that P(Lys) has toxicity.

After the rats were killed with an overdose of sodium pentobarbital, the eyes were immediately enucleated, snap-frozen in OCT compound 1, 4, 8, 24, and 168 h later for the PIC micelle group ($n = 4$ at each time point) and 1 h later for the FITC P(Lys) group ($n = 3$). Then frozen sections were mounted with the ProLong Antifade Kit (Molecular Probes, Eugene, OR, USA) and observed under a fluorescent microscope (model IX, Olympus, Tokyo, Japan).

2.5. Measurement of the concentration of PIC micelle in laser-treated eyes and blood

To investigate the concentration of FITC-P(Lys) in laser-treated eyes and blood, rats received PIC micelle encapsulating FITC-

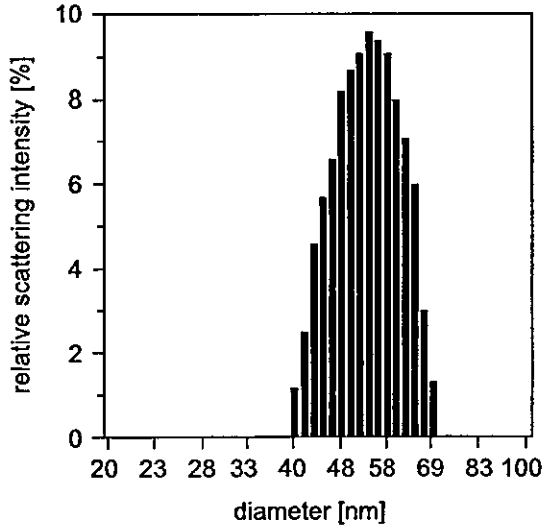

Fig. 2. DLS histogram of PIC micelle encapsulating FITC-P(Lys). The average diameter and polydispersity index of PIC micelles were evaluated by DLS measurement at 25°C, using a light scattering spectrophotometer. PIC micelle was narrowly dispersed with a size around 50.7 nm.

P(Lys) ($n=20$) or free FITC-P(Lys) ($n=3$) intravenously 7 days after photocoagulation. They were killed with an overdose injection of sodium pentobarbital 1, 4, 8, 24 and 168 h after receiving the PIC micelles encapsulating FITC-P(Lys) ($n=4$ at each time point) and 1 h after receiving free FITC-P(Lys) ($n=3$). Immediately after death, blood samples were collected and the eyes were enucleated. The blood samples were centrifuged at 12000 rpm for 5 min and the supernatant was collected and subjected to spectrophotometric analysis. The retina/choroid was collected after the anterior segment and vitreous were removed. Then, the retina/choroid samples were homogenized in 0.1 ml of PBS and suspended in a total of 0.3 ml of PBS. The homogenates were then centrifuged at 12000 rpm for 5 min and the supernatant was collected and subjected to spectrophotometric analysis. The fluorescence intensity was measured in a fluorescence spectrophotometer (FP-6500, Jasco, Tokyo, Japan) with an excitation wavelength of 495 nm and an emission wavelength of 520 nm. The actual concentration of FITC-P(Lys) was calculated by means of a calibration curve.

2.6. Statistical analysis

Mann–Whitney's *U*-test was used. Values of $P<0.05$ were considered statistically significant.

3. Results

3.1. Preparation of PIC micelle encapsulating FITC-P(Lys)

Precipitation after mixing FITC-P(Lys) and PEG-P(Asp) solutions at 25°C was not observed, even after a period of over 2 months, suggesting the high storing stability of PIC micelle. Fig. 2 shows the size distribution of PIC micelle obtained from histogram analysis of DLS measurements. It was clear that the prepared PIC micelle had a unimodal size distribution. Also the average diameter and polydispersity index of PIC micelle were determined to be 50.7 nm and 0.046 by using the cumulant approach of DLS measurement, indicating the formation of PIC micelle with an extremely narrow size distribution.

3.2. Accumulation of PIC micelle to CNV lesions

3.2.1. PIC micelle group. Fluorescent staining was observed in the CNV lesions and also in the choriocapillaris

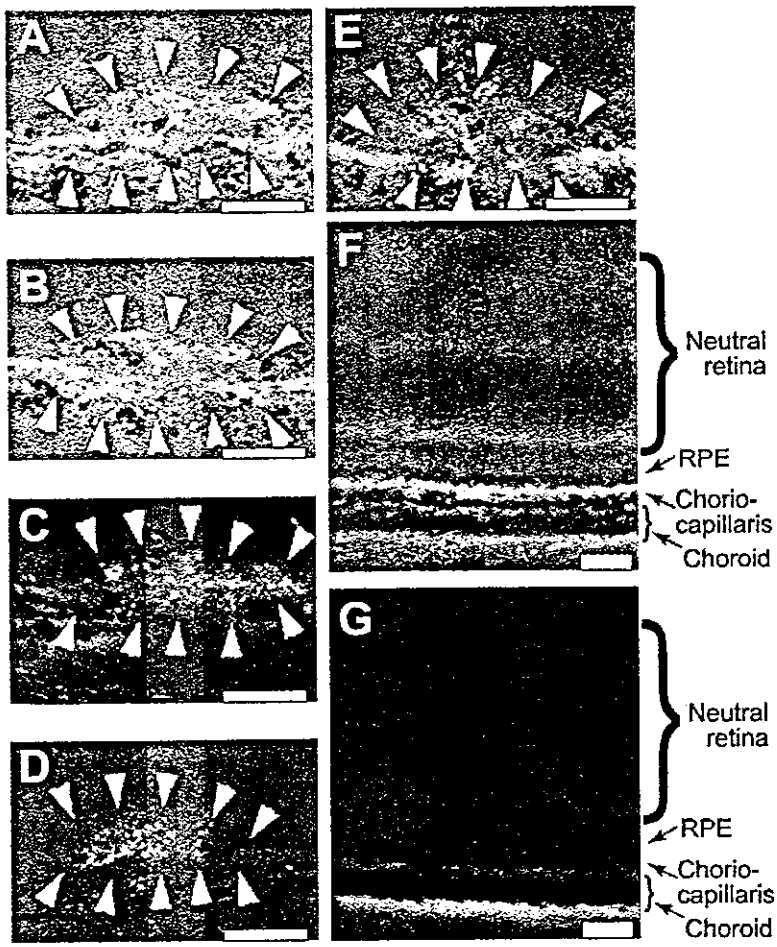

Fig. 3. Accumulation of PIC micelle to CNV lesion. The frozen sections of the CNV lesions were observed under a fluorescent microscopic 1 (A), 4 (B), 24 (C) and 168 (D) h after rats received PIC micelle-incorporated FITC-P(Lys). Note that FITC-P(Lys) initially diffuses to the CNV lesion and choriocapillaris (A,B), and becomes confined to the CNV lesion thereafter (C,D). Bright fluorescence was observed in the CNV lesions up to 168 h (D). One hour after rats received an intravenous injection of free FITC-P(Lys), FITC-P(Lys) distributes to the CNV lesion and choriocapillaris (E). Arrowheads in A–E indicate CNV lesions. Most rats died 1 h after free FITC-P(Lys) administration. In the laser-non-treated eyes, fluorescence was observed in the choriocapillaris 1 h after rats received PIC micelle (F) and the fluorescence became invisible 4 h after the injection of PIC micelle (G). Note that PIC micelle effectively accumulated to the CNV lesion throughout the studied period. Scale bar, 25 μm.

for up to 4 h (Fig. 3A,B). Twenty-four hours after the administration, accumulation of FITC-P(Lys) to the CNV lesion was more evident and fluorescence became invisible outside the photocoagulated lesion including the choroidal and retinal vasculature (Fig. 3C). The fluorescence was observed for up to 168 h (Fig. 3D). In the non-laser-treated eyes, the fluorescence was visible in the choroidal vessels for up to 4 h (Fig. 3F), and the fluorescence became invisible at 24 h and thereafter (Fig. 3G and data not shown). Light microscopic analysis revealed no abnormalities in other retinal structures.

3.2.2. Free FITC-P(Lys) group. Most rats died 1 h after the FITC-P(Lys) administration. When evaluated 1 h after intravenous administration, fluorescence was observed in the CNV lesion and choriocapillaris (Fig. 3E). In order to reduce the toxic effect of free FITC-P(Lys), rats received a lower dose (10 mg per injection) of free FITC-P(Lys). However, all rats died before 2 h after the administration ($n > 10$).

3.3. Concentration of FITC-P(Lys) in the laser-treated eyes

3.3.1. PIC micelle group. FITC-P(Lys) was detected in the retina/choroid from the laser-treated eyes as early as 1 h and the concentration peaked at 4 h and the residual FITC-P(Lys) was still evident 168 h after intravenous administration (Fig. 4). The concentration of FITC-P(Lys) was below the detectable level in the non-laser-treated eyes.

3.3.2. Free FITC-P(Lys) group. When evaluated 1 h after intravenous administration, the concentration of FITC-P(Lys) in the free FITC-P(lys) group was significantly lower compared to that in the PIC micelle group (Fig. 4).

3.4. Concentration of PIC micelle in blood

Fig. 5 shows the concentration of FITC-P(Lys) in blood after a single injection of either free FITC-P(Lys) or PIC micelle encapsulating FITC-P(Lys). The residual amount of FITC-P(Lys) in blood was 5.0, 7.8, 3.8 and 0.5% of the injected dose at 1, 4, 8, and 24 h, respectively, after intravenous injection of PIC micelles encapsulating FITC-P(Lys). After 168 h, it was below the detectable level. The concentration of FITC-P(Lys) in blood was 15% of the injected dose 1 h after free FITC-P(Lys) injection.

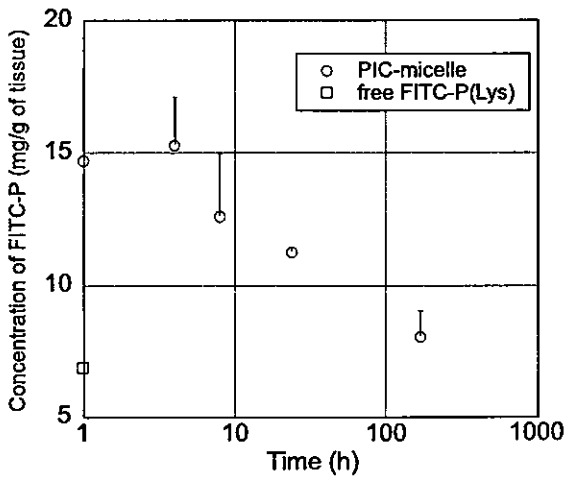

Fig. 4. Concentration of FITC-P(Lys) in retina/choroid. Concentrations of FITC-P(Lys) in retina/choroid after rats received equivalent doses of FITC-P(Lys) of PIC micelle-incorporated FITC-P(Lys). Note that FITC-P(Lys) was detected in retina/choroid from the laser-treated eyes of the PIC micelle group as early as 1 h and the concentration peaked at 4 h and was still evident 18 h after intravenous administration, whereas the concentration of FITC-P(Lys) in the free FITC-P(Lys) group was significantly lower compared to that in the PIC micelle group 1 h after injection. Most rats died 1 h after free FITC-P(Lys) administration. Error bars indicate S.D.

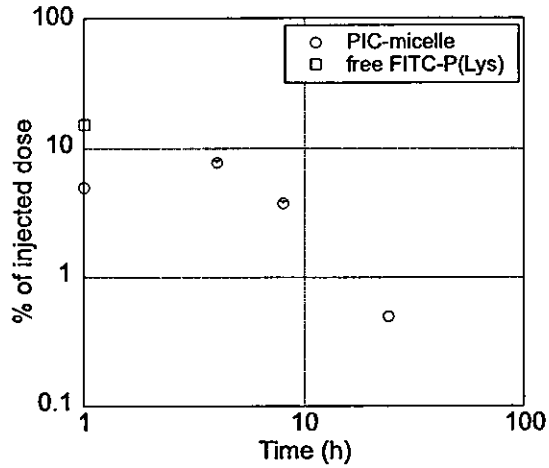

Fig. 5. Concentration of PIC micelle in blood. Concentration of FITC-P(Lys) in blood after rats received 400 μl of free FITC-P(Lys) at a concentration of 5.0 mg/ml or 400 μl of PIC micelles encapsulating 5.0 mg/ml FITC-P(Lys). The residual amount of FITC-P(Lys) in blood was 5.0, 7.8, 3.8 and 0.5% of the injected dose at 1, 4, 8 and 24 h, respectively, after intravenous injection of PIC micelles encapsulating FITC-P(Lys). Most rats died 1 h after free FITC-P(Lys) administration, whereas no rats died after intravenous injection of PIC micelles encapsulating FITC-P(Lys). Error bars indicate S.D.

4. Discussion

In this study, FITC-P(Lys) was retained in the CNV lesion for as long as 168 h after intravenous injection of PIC micelle encapsulating FITC-P(Lys) as demonstrated by histological analysis and confirmed by the measurement of the concentration in the retina/choroid of the laser-treated eyes. Because it was impossible to distinguish free FITC-P(Lys) and FITC-P(Lys) encapsulated into PIC micelle, the data presented here do not address whether FITC-P(Lys) was present in a free form or encapsulated in the PIC micelle. Together with the high mortality rate associated with free FITC-P(Lys) administration, it was not directly proven whether encapsulation of FITC-P(Lys) into PIC micelle enhanced the accumulation of FITC-P(Lys) to the CNV lesions throughout the studied period. However, it was demonstrated that a significantly higher amount of FITC-P(Lys) accumulated to the CNV lesions 1 h after the injection in the PIC micelle group compared to the free FITC-P(Lys) group. It is of note that the amount of FITC-P(Lys) in the non-laser-treated eyes was below the detectable level. In addition, because CNVs are highly permeable similar to the newly formed vessels in solid tumors, it is plausible to speculate that the PIC micelle is likely to accumulate to CNV lesions presumably through the EPR effect. This idea is consistent with recent studies that have demonstrated that macromolecules accumulate in the CNV lesion in rabbits [18].

We have reported that polymeric micelles have long-circulating characteristics [8] and that the stability of PIC micelles

in the blood stream can be controlled by the charge ratio and the length of the poly-amino acid, one of the block copolymers that constitute PIC micelles [19]. In this study, 0.5% of the injected dose was retained in the blood even 24 h after injection of PIC micelle encapsulating FITC-P(Lys). Generally, the concentration of compounds in the blood decreases rapidly to less than 0.1% of the injected dose in a few hours after intravenous injection of low molecular weight compounds such as fluorescein sodium. In fact, the concentration of fluorescein sodium 1 h after intravenous injection was at a non-detectable level (data not shown). Taken together, PIC micelle encapsulating FITC-P(Lys) also have long-circulating characteristics, which is a great advantage to exert the EPR effect.

The concentration of FITC-P(Lys) delivered by PIC micelle to the retina/choroid peaked 4 h after injection, and remained as long as 7 days at a concentration higher than 15 μg/g protein after only one intravenous injection. Because a total of 2 mg FITC-P(Lys) was administered, the total amount of FITC-P(Lys) was approximately 300 ng in the retina/choroid when it was delivered by PIC micelles. As deduced from these results, 0.02% of the injected dose accumulated to and was retained within the retina/choroid for as long as 7 days. In the blood, 5% and 0.5% of the injected dose were retained 1 and 24 h after the injection of PIC micelle, respectively. Thus, the FITC-P(Lys) in blood vs. that in the retina/choroid at 1 and 24 h after the injection was 340:1 and 45:1, respectively, suggesting that PIC micelle could be effectively targeted to the retina/choroid through the EPR effect, in spite of the low concentrations in blood. Moreover, we found that the administration of free FITC-P(Lys) was associated with high mortality, whereas administration of PIC micelles encapsulating FITC-P(Lys) was not. This is in line with previous studies which demonstrated that modification of compounds with a polymeric carrier results in a decreased adverse effect [20]. Our observation supports that the PIC micelle attenuated the adverse effect, although the underlying cause of this lethal toxicity remains to be unraveled. Such characteristics of the PIC micelle are a great advantage to achieve effective targeting of drug while reducing systemic adverse effects.

The concentration of PIC micelles increased in the liver and spleen but gradually decreased in the kidney and lung within 24 h after intravenous injection (data not shown), suggesting that the PIC micelle is mainly eliminated through the spleen.

In summary, it has been demonstrated that the PIC micelle effectively accumulates to the CNV lesion. The distribution of drug-loaded polymeric micelles in the body may be determined mainly by their size and surface properties and is less affected by the properties of loaded drugs if they are embedded in the inner core of the micelles. Since PIC micelles are demonstrated to be able to reserve a variety of drugs, enzymes [21] and DNA in the core and can serve as non-viral gene delivery vectors [9,19,22], we believe that PIC micelles have great potential for achieving effective drug targeting to CNV.

References

[1] Ferris III, F.L., Fine, S.L. and Hyman, L. (1984) Arch. Ophthalmol. 102, 1640–1642.
[2] Bressler, N.M., Bressler, S.B. and Fine, S.L. (1988) Surv. Ophthalmol. 32, 375–413.
[3] Macular Photocoagulation Study Group (1991) Arch. Ophthalmol. 109, 1242–1257.
[4] Treatment of age related macular degeneration with photodynamic therapy (TAP) Study Group (1999) Arch. Ophthalmol. 117, 1329–1345.
[5] Ciulla, T.A., Danis, R.P. and Harris, A. (1998) Surv. Ophthalmol. 43, 134–146.
[6] Hunt, D.W. and Margaron, P. (2003) IDrugs 6, 464–469.
[7] Kimura, H., Yasukawa, T., Tabata, Y. and Ogura, Y. (2001) Adv. Drug Deliv. Rev. 52, 79–91.
[8] Kataoka, K., Harada, A. and Nagasaki, Y. (2001) Adv. Drug Deliv. Rev. 47, 113–131.
[9] Kakizawa, Y. and Kataoka, K. (2002) Adv. Drug Deliv. Rev. 54, 203–222.
[10] Matsumura, Y. and Maeda, H. (1986) Cancer Res. 46, 6387–6392.
[11] Nakanishi, T. et al. (2001) J. Control. Release 74, 295–302.
[12] Nishiyama, H., Kato, Y., Sugiyama, Y. and Kataoka, K. (2001) Pharm. Res. 18, 1035–1041.
[13] Kataoka, K., Matsumoto, T., Yokoyama, M., Okano, T., Sakurai, Y., Fukushima, S., Okamoto, K. and Kwon, G.S. (2000) J. Control. Release 64, 143–153.
[14] Nishiyama, N. and Kataoka, K. (2003) Adv. Exp. Med. Biol. 519, 155–177.
[15] Harada, A. and Kataoka, K. (1995) Macromolecules 28, 5294–5299.
[16] Yanagi, Y., Tamaki, Y., Obata, R., Muranaka, K., Homma, N., Matsuoka, H. and Mano, H. (2002) Invest. Ophthalmol. Vis. Sci. 43, 3495–3499.
[17] Yanagi, Y., Tamaki, Y., Inoue, Y., Obata, R., Muranaka, K. and Homma, N. (2003) Invest. Ophthalmol. Vis. Sci. 44, 751–754.
[18] Yasukawa, T., Kimura, H., Tabata, Y., Miyamoto, H., Honda, Y., Ikada, Y. and Ogura, Y. (1999) Invest. Ophthalmol. Vis. Sci. 40, 2690–2696.
[19] Harada-Shiba, M., Yamauchi, K., Harada, A., Takamisawa, I., Shimokado, K. and Kataoka, K. (2002) Gene Ther. 9, 407–414.
[20] Mizumura, Y. et al. (2001) Jpn. J. Cancer Res. 92, 328–336.
[21] Harada, A. and Kataoka, K. (2001) J. Control. Release 72, 85–91.
[22] Harada, A., Togawa, H. and Kataoka, K. (2001) Eur. J. Pharm. Sci. 13, 35–42.

THE JOURNAL OF GENE MEDICINE
J Gene Med 2004; 6: 76–84.
Published online in Wiley InterScience (www.interscience.wiley.com). DOI: 10.1002/jgm.470

RESEARCH ARTICLE

In situ single cell observation by fluorescence resonance energy transfer reveals fast intra-cytoplasmic delivery and easy release of plasmid DNA complexed with linear polyethylenimine

Keiji Itaka[1,2]
Atsushi Harada[1]
Yuichi Yamasaki[1]
Kozo Nakamura[2]
Hiroshi Kawaguchi[2]
Kazunori Kataoka[1]*

[1]*Department of Materials Science and Engineering, Graduate School of Engineering, The University of Tokyo, 7-3-1 Hongo, Bunkyo-ku, Tokyo 113-8656, Japan*

[2]*Department of Orthopaedic Surgery, Faculty of Medicine, The University of Tokyo, 7-3-1 Hongo, Bunkyo-ku, Tokyo 113- 8655, Japan*

*Correspondence to:
Professor Kazunori Kataoka, Department of Materials Science and Engineering, Graduate School of Engineering, The University of Tokyo, 7-3-1 Hongo, Bunkyo-ku, Tokyo 113-8656, Japan.
E-mail:
kataoka@bmw.t.u-tokyo.ac.jp

Received: 9 May 2003
Revised: 11 July 2003
Accepted: 11 July 2003

Abstract

Background The investigation into the intracellular mechanisms for gene expression has acquired great impetus for the improvement of the transfection efficiency by a non-viral gene delivery system.

Methods Intracellular trafficking as well as release of plasmid DNA (pDNA) complexed with polycations, including linear and branched polyethylenimine (LPEI, BPEI) and poly(L-lysine) (PLL), were explored under confocal microscopy using fluorescence resonance energy transfer (FRET) between a pair of donor–acceptor fluorescent dyes (fluorescein and Cy3) tagged on a single pDNA molecule.

Results pDNA complexed with LPEI underwent a rapid escape from the endosomes, spreading uniformly into the cytoplasm with a substantial decrease in FRET efficiency due to the disintegration of LPEI/pDNA polyplex structure. pDNA complexed with BPEI also achieved a rapid escape from the endosomes. Nevertheless, the pDNA retained high FRET efficiency even after 24 h, indicating an appreciable stability of the BPEI/pDNA polyplex to keep pDNA in a condensed state. In the PLL/pDNA polyplexes, neither endosome escape nor pDNA decondensation was observed. These intracellular characteristics of polyplexes showed a clear correlation to their gene transfection efficiency: The LPEI/pDNA revealed a considerably higher and faster gene expression compared with BPEI/pDNA. Atomic force microscopy revealed that BPEI induced more effective condensation of pDNA than LPEI, being consistent with restricted cytoplasmic release of complexed pDNA.

Conclusion Fast endosomal escape and subsequent smooth disintegration of LPEI/pDNA in the cytoplasm are likely to be determining factors for the excellent transfection efficiency of this polyplex system. These properties may be particularly beneficial to achieve appreciably high gene expression in a prompt manner. Copyright © 2004 John Wiley & Sons, Ltd.

Keywords polyethylenimine; DNA; fluorescence resonance energy transfer; confocal microscopy; transfection; nucleic acid conformation

Introduction

Improvement of transfection efficiency is one of the most important subjects for the development of a non-viral gene delivery system. For this purpose,